



Published in final edited form as:

Exp Neurol. 2020 January ; 323: 113072. doi:10.1016/j.expneurol.2019.113072.

Mechanism and role of the intra-axonal Calreticulin translation in response to axonal injury

Almudena Pacheco^{1,*}, Tanuja Merianda², Jeffery L. Twiss³, Gianluca Gallo¹

¹Temple University School of Medicine, Shriners Pediatric Research Center, Department of Anatomy and Cell Biology, 3500 North Broad St, Philadelphia, PA 19140

²Drexel University, Department of Biology, Philadelphia, Pennsylvania 19104

³University of South Carolina, Department of Biological Sciences, Columbia 29208 SC, USA

Abstract

Following injury, sensory axons locally translate mRNAs that encode proteins needed for the response to injury, locally and through retrograde signaling, and for regeneration. In this study, we addressed the mechanism and role of axotomy-induced intra-axonal translation of the ER chaperone Calreticulin. *In vivo* peripheral nerve injury increased Calreticulin levels in sensory axons. Using an *in vitro* model system of sensory neurons amenable to mechanistic dissection we provide evidence that axotomy induces local translation of Calreticulin through PERK (protein kinase RNA-like endoplasmic reticulum kinase) mediated phosphorylation of eIF2 α by a mechanism that requires both 5' and 3'UTRs (untranslated regions) elements in Calreticulin mRNA. ShRNA mediated depletion of Calreticulin or inhibition of PERK signaling increased axon retraction following axotomy. In contrast, expression of axonally targeted, but not somatically restricted, Calreticulin mRNA decreased retraction and promoted axon regeneration following axotomy *in vitro*. Collectively, these data indicate that the intra-axonal translation of Calreticulin in response to axotomy serves to minimize the ensuing retraction, and overexpression of axonally targeted Calreticulin mRNA promotes axon regeneration.

Graphical Abstract

*Corresponding author: Almudena Pacheco (almudena.pacheco@temple.edu).

Authors contributions

Almudena Pacheco: Conceived and designed the study, performed the experiments, analyzed and interpreted the data, wrote the paper.

Tanuja Merianda: Performed the *in vivo* experiments.

Jeffery L. Twiss: Conception of the study, interpretation of data, revising the article.

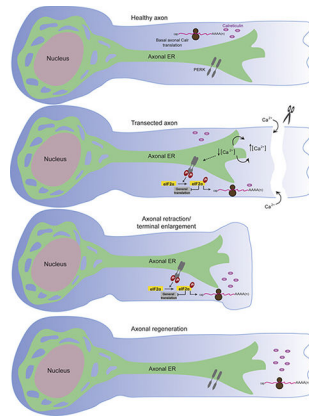
Gianluca Gallo: Interpretation of data, revising and edits to the article.

All authors have approved the final article.

Competing interests

"Declarations of interest: none"

Publisher's Disclaimer: This is a PDF file of an unedited manuscript that has been accepted for publication. As a service to our customers we are providing this early version of the manuscript. The manuscript will undergo copyediting, typesetting, and review of the resulting proof before it is published in its final form. Please note that during the production process errors may be discovered which could affect the content, and all legal disclaimers that apply to the journal pertain.



Keywords

Axonal injury; Calreticulin; translational control; eIF2 α phosphorylation

Introduction

Injury of adult peripheral neurons is followed by spontaneous axon regeneration (Bradke et al., 2012). The intrinsic growth capacity of PNS axons is higher than CNS axons that do not spontaneously regenerate after injury (Chierzi et al., 2005). Extensive effort has been devoted to understanding the mechanisms that explains these differences. Compared with CNS axons, peripheral axons contain higher levels of ribosomal proteins and translation elongation factors at all developmental stages (Verma et al., 2005; Zheng et al., 2001). There are several studies from DRG neurons demonstrating the axonal mRNA localization and local translation after conditioning-injury (Willis et al., 2005; Zheng et al., 2001). The regenerative ability of PNS axons depends on their capacity to locally synthesize new proteins and degrade others at the injury site autonomously from the cell body (Gumy et al., 2010). For example, nerve injury triggers translation of axonal mRNAs whose encoded proteins are needed to stimulate transcriptional responses in the neuronal cell body (Hanz et al., 2003; Perlson et al., 2005; Yudin et al., 2008) and other locally synthesized proteins contribute to growth cone formation after axotomy (Verma et al., 2005). *Cis*-elements in the UTRs of axonally localized mRNAs play central roles in post-transcriptional regulation through subcellular mRNA localization, translational efficiency, and/or mRNA stabilization (Andreassi and Riccio, 2009; Chatterjee and Pal, 2009). The 5'UTR elements are most often linked to translation regulation (Bi et al., 2007; Choi et al., 2018; Vuppalanchi et al., 2012) and the 3'UTRs regions are critical both for the targeting of mRNAs to specific subcellular compartments and in some cases for translational control (Andreassi and Riccio, 2009; Huttelmaier et al., 2005; Tushev et al., 2018). Protein synthesis can be regulated globally during stress by modulating the activity of the translation initiation factor (eIFs) (Spriggs et al., 2010). For example, activation of PERK leads to eIF2 α phosphorylation at Ser51 impeding translational initiation as part of the integrated stress response (Pakos-Zebrucka et al., 2016). PERK is a type I ER membrane protein containing a stress-sensing domain in the lumen of the ER, a transmembrane segment, and a cytosolic kinase domain (Shi et al.,

1998). ER stress activates PERK via oligomerization and autophosphorylation at multiple serine, threonine, and tyrosine residues (Ma et al., 2002; Su et al., 2008).

Calreticulin is a pleiotropic protein that functions in the ER as a molecular chaperone involved in the folding process for nascent proteins as well as in the homeostatic control of cytosolic and ER calcium levels (Michalak et al., 1998; Michalak et al., 2002; Ostwald and MacLennan, 1974). Previous work has established that Calreticulin mRNA (Calr) is locally translated in isolated sensory axons in response to ER stress and ER calcium release (Vuppalanchi et al., 2012). Calreticulin mRNA contains two *cis*-elements in the 3'UTR. A proximal 3' UTR *cis*-element that confers stimulus-dependent transport and a second more distal element that confers its constitutive transport into PNS and CNS axons (Vuppalanchi et al., 2010; Willis et al., 2007). The 5'UTR of Calreticulin mRNA further confers translational regulation through phosphorylation of eIF2 α at serine 51 in response to ER calcium release (Vuppalanchi et al., 2012). In this study, we observed an increase of axonal Calreticulin translation in response to axonal injury. Little is known about the post-transcriptional mechanisms that regulate axonal mRNA translation during injury signaling and the diversity of inputs that trigger eIF2 α kinase activation in neurons has not been fully elaborated. In this study, we have used an acute injury (axotomy) and a physiological stress stimulus (LPA) to examine the effects of PERK-eIF2 α phosphorylation in axonal Calreticulin translation. We presented evidence that both axotomy and LPA enhance axonal translation of Calreticulin mRNA through PERK-eIF2 α phosphorylation and through concerted roles of both Calreticulin 5'UTR and 3'UTR elements. The data indicate that axonal Calreticulin translation is rapidly triggered after injury through PERK-eIF2 α phosphorylation to regulate the ensuing axonal retraction and promote elongation during axonal regeneration.

Results

Axonal Calreticulin levels increase in response to injury

Calreticulin functions as a molecular chaperone in the ER and in calcium homeostasis through its very high calcium binding affinity (Michalak et al., 1998; Michalak et al., 2002; Ostwald and MacLennan, 1974). Calcium influx in the axoplasm represents a fast signaling event in response to injury that is able to trigger several mechanisms connected to axonal growth ranging from local activation of proteases needed for growth cone formation to retrograde signaling (Cho and Cavalli, 2014; Kamber et al., 2009). Calreticulin protein and mRNA localize into axons of cultured DRG neurons *in vitro* and into PNS axons *in vivo* (Vuppalanchi et al., 2010; Willis et al., 2005) and the upregulation of ER stress markers has been correlated with *in vivo* regenerative responses to axotomy (Onate et al., 2016). We asked whether sciatic nerve crush injury alters axonal Calreticulin protein levels. Sciatic nerves sections (naïve and injured) were collected at 1 h, 6 h, 18 h and 7 days after crush injury and immunostained. An increase in axonal Calreticulin protein levels was apparent at 6 h post-injury and reached maximum values 18 h post-injury compared with the control, naïve sciatic nerve (Fig. 1 A and 1B). Thus, axotomy rapidly increases axonal Calreticulin protein levels in the PNS.

Since eIF2 α phosphorylation was shown to increase translation of Calreticulin in axons of cultured DRG neurons (Vuppalanchi et al., 2012), we aimed to analyze the signaling pathway responsible for rapidly increased axonal Calreticulin protein levels after axotomy. Chick DRG explants were used as an *in vitro* model system where we could simultaneously sever many axons at once at a predetermined distance from the DRG soma (Spillane et al., 2012). 24 hour explant cultures of embryonic day (E) 8 chicken DRG explants were subjected to manual axotomy at $\sim 800 \mu\text{m}$ from the soma as outlined in the Materials and Methods section (Fig. 2A). These cultures were fixed 20 min later and immunostained for phospho-eIF2 α (eIF2 α -pS51) (Kimball, 1999) and Calreticulin. Phosphorylation of eIF2 α on Ser51 (eIF2 α -pS51) inhibits general cap-dependent translation initiation to favor cap-independent translation but also results in a paradoxical increase in translation of some mRNAs through cap-dependent mechanisms. Axonal immunoreactivity for both eIF2 α -pS51 (Fig. 2B and 2C) and Calreticulin (Fig. 2D and 2E) significantly increased in the distal end of the severed axon, maintaining continuity with the cell body, proximal to the cut site. Axotomy increases axoplasmic Ca²⁺ and depletes ER Ca²⁺ stores of ER in sensory neurons (Rigaud et al., 2009). The decrease in ER Ca²⁺ levels activate PERK that subsequently phosphorylate eIF2 α on Ser 51 (Harding et al., 1999; Raven and Koromilas, 2008). Consistent with this, axonal eIF2 α -pS51 and Calreticulin levels after axotomy were significantly lower in axons of DRG explants that were pre-treated with the PERK inhibitor GSK2606414 (90 μM) (Axten et al., 2012) (Fig. 2B and 2D). In agreement with previous work in axotomized DRG spot cult cultures (Ohtake et al., 2018), the fluorescence signal of phospho-PERK was also increased after axotomy (Supplemental figure 1) indicating the activation of PERK in response to injury. Thus, axotomy could be increasing eIF2 α -pS51 and subsequently Calreticulin protein levels by locally activating PERK, which has been shown to localize to DRG axons (Wang et al., 2007). Taken together, these results suggest that axotomy triggers synthesis of new Calreticulin proximal to the injury site through activation of PERK and subsequent eIF2 α phosphorylation.

Axonal injury triggers local Calreticulin translation

Axotomy-induced increase in intra-axonal Ca²⁺ levels has been shown to be required for translation of axonal mRNAs that encode proteins needed to assemble retrograde injury signaling complexes (Perry and Fainzilber, 2009) and for new growth cone formation (Vogelaar et al., 2009). We considered whether the rapid localized translation of Calreticulin mRNA represents a similarly fast signaling response to injury. In order to study the mechanisms underlying the injury-induced increase in axonal Calreticulin levels, we utilized an *in vitro* model system that allows for detailed spatial-temporal analysis of translational regulation in DRG neurons using a diffusion-limited reporter as a surrogate for endogenous mRNAs. Dissociated adult rat DRG neurons were transfected with constructs for expression of diffusion limited myristoylated (*Myr*) GFP carrying the Calr 3'UTR (3'Calr) for axonal localization and the Calr 5'UTR (5'Calr) for translational regulation (5'Calr-*Myr*GFP-3'Calr) (Vuppalanchi et al., 2012). The myristoylation domain restricts diffusion of the GFP protein product in the axonal compartment, providing a measure of localized protein synthesis over short duration time lapse experiments using fluorescence recovery after photobleaching (FRAP) as previously reported (Aakalu et al., 2001; Vuppalanchi et al., 2010; Yudin et al., 2008). Single axons were cut at 50–100 μm from the axon tip using a

pulled glass electrode (Chierzi et al., 2005) and then recovery of GFP signals was monitored over 35 min in the distal end of the severed axon, maintaining continuity with the cell body, proximal to the cut site (Fig. 3A, white arrow). The recovery of the fluorescence signal along axotomized axons was significantly increased (> 80%) at 20 min after axotomy compared to the control axons not axotomized (Fig. 3A and 3B). This increase in axonal GFP signal was significantly diminished by the translational inhibitor cycloheximide (Chx) demonstrating that signal recovery was due to protein synthesis (Fig. 3B).

Since PERK inhibition diminished the axotomy-induced increase of endogenous axonal Calreticulin protein (Fig. 2D and 2E), we asked if PERK activation is required for the increase in 5'Calr-MyrGFP-3'Calr translation after *in vitro* axotomy. For this, we pretreated DRG cultures expressing 5'Calr-MyrGFP-3'Calr with GSK2606414 to inhibit PERK and then analyzed axonal MyrGFP recovery in axons proximal to cut site. PERK inhibition significantly decreased axonal 5'Calr-MyrGFP-3'Calr fluorescence recovery compared to axotomized DRG neurons not treated with PERK inhibitor (Fig. 3C and 3D). To determine PERK's contribution to basal translation of 5'Calr-MyrGFP-3'Calr mRNA, we analyzed the effect of the PERK inhibitor in the fluorescence recovery of distal axons without being first injured. GSK2606414 did not alter the basal translation of 5'Calr-MyrGFP-3'Calr mRNA (compare Fig. 3B no axotomy and Fig. 3D no axotomy + PERKi, see analysis in legend of figure 3). Taken together, these data suggest that axotomy of DRG neurons triggers axonal Calreticulin translation in a PERK dependent manner.

Axotomy increases eIF2 α phosphorylation in axons of DRG neurons with subsequent translation of Calreticulin mRNA in axons (Fig. 2B–C and Fig. 3). Previous studies have shown that Calr 5'UTR confers translational control through a mechanism that requires eIF2 α phosphorylation (Vuppalanchi et al., 2012). To test the role of Calr 5'UTR in injury-induced Calreticulin mRNA translation, we replaced Calr 5'UTR with that of Actb (5'Actb-MyrGFP-3'Calr). Actb mRNA extends into axonal growth cones of developing cortical neurons (Bassell et al., 1998) and into axonal process of DRG neurons where is translated (Zheng et al., 2001). Importantly, we saw no significant GFP fluorescence recovery in axons of DRG neurons expressing an mRNA where Calr 5'UTR was replaced with that of Actb (5'Actb-MyrGFP-3'Calr) relative to the non-axotomized axons (Fig. 4A–B). These current data suggest that axotomy induced increase in axonal Calreticulin translation requires the RNA motifs in its 5'UTR.

The 3'UTR of Calreticulin mRNA drives axonal localization into the distal axons of DRG neurons (Vuppalanchi et al., 2010). To test the possibility that Calr 3'UTR impacts axonal Calreticulin translational regulation in response to injury, we replaced Calr 3'UTR with that of Hmgb1 (5'Calr-MyrGFP-3'Hmgb1). Hmgb1 mRNA is constitutively transported into axons of cultured DRG neurons (Willis et al., 2007) and its 3'UTR is sufficient for axonal localization of heterologous reporter mRNA (Donnelly et al., 2013), so the 5'Calr-MyrGFP-3'Hmgb1 mRNA would be transported and locally translated in DRG axons. We saw no significant GFP fluorescence recovery in axons of DRG neurons expressing an mRNA where Calr 3'UTR was replaced with that of Hmgb1 (5'Calr-MyrGFP-3'Hmgb1) relative to the non-axotomized axons (Fig. 4C–D). These current data suggest that axotomy induced increase in axonal Calreticulin translation requires the RNA motifs in its 3'UTR.

PERK is required for the increase of axonal Calreticulin translation in response to ER stress

LPA is a bioactive phospholipid that mediates multiple cellular responses (Moolenaar et al., 2004) *some of them resembling a series of processes undergoing after axonal injury*. Axotomy depletes ER- Ca^{2+} stores (Rigaud et al., 2009) and leads to an elevation of axoplasmic and cell body Ca^{2+} that is necessary for axon regeneration (Bradke et al., 2012). In DRG neurons, LPA increases intracellular calcium concentration through Ca^{2+} mobilization from intracellular stores (Elmes et al., 2004) and can cause protease activation, cytoskeletal rearrangements, and neurite retraction in neural cell lines and primary neurons (Campbell and Holt, 2001; N. Fukushima, 2011; Ye et al., 2002). The ER Ca^{2+} released during ER stress results in ER luminal signals that activate PERK with the consequent phosphorylation of eIF2 α Ser 51 (Harding et al., 2002; Harding et al., 1999). LPA treatment increase eIF2 α phosphorylation in axons of DRG neurons followed by axonal Calreticulin mRNA translation (Vuppalanchi et al., 2012). PERK has been detected in DRG axons (Wang et al., 2007) and we have shown that the inhibition of this kinase prevents the increase of axonal Calreticulin translation in response to injury (Fig. 3C–3D). Since LPA triggers ER Ca^{2+} release (Elmes et al., 2004), a Ca^{2+} -dependent activation of axonal PERK may lead to phosphorylation of eIF2 α and translation of axonal Calreticulin mRNA under LPA treatment. To test this hypothesis we generated a shRNA expression plasmid to target rat PERK sequence (NM_031599.2) (pSUPERshRNA-PERK-GFP). Determination of siRNA mediated endogenous PERK knockdown was performed through western blot of lysates collected 48 h after transfection of rat hybridoma F11 cells with pSUPERshRNA-PERK-GFP. The expression of shRNA-PERK efficiently knocked down the endogenous PERK (compare lane 3 with lanes 1 and 2) (Fig. 5A). We generated constructs for PERK that encoded an in frame C-terminal BFP with the coding sequence of PERK (Eif2ak3; NC_000072), or kinase dead K618A Lys 618 to Ala mutant (Harding et al., 1999) (pPERK_{wt}-BFP and pPERK_{KD}-BFP, respectively) versus the same construct engineered to be resistant to the siRNA target sequence (pPERK_{wt}rescue-BFP and pPERK_{KD}rescue-BFP, respectively). Western blot of lysates from pSUPERshRNA-PERK-GFP transfected HEK 293 cells (Fig. 5B) show that the shRNA effectively knocked down PERK protein expression from both constructs expressing the *wt* and *KD* PERK sequences (lanes 2 and 5) in compare with the control co-transfected with the shRNA-nontarget, (lanes 1 and 4). The PERK levels were rescued by co-transfecting the cells with pPERK_{wt}rescue-BFP and pPERK_{KD}rescue-BFP (compare lane 3 with 2 and lane 6 with 5) (Fig. 5B). The expression of pSUPER-shPERK-GFP in DRG neurons was determined by the presence of GFP expression (Fig. 5C, right panel). DRG neurons were co-transfected with the plasmids that express the shRNA-PERK (pSUPERshRNAPERK-GFP) plus the plasmid that express the mRNA 5'Calr-*Mymcherry*-3'Calr (left panel, Fig. 5C) and cultured for 48 h before imaging analysis. By FRAP analyses, recovery of 5'Calr-*Mymcherry*-3'Calr fluorescence in LPA-treated DRG cultures was significantly increased in the distal axons of DRG neurons expressing non-targeting shRNA in compare with the *not LPA-treated control neurons expressing non-targeting shRNA*. However, the recovery of 5'Calr-*Mymcherry*-3'Calr fluorescence in LPA-treated DRG cultures was significantly reduced in the distal axons of DRG neurons expressing shRNA-PERK in comparison with the control neurons expressing non-targeting shRNA and basal levels of PERK (Fig. 5C–D). This indicates that PERK is

required for the axonal translation of Calreticulin in response to LPA. To rule out the possibility of off target effects of the shRNA-PERK, we co-transfected the cells with the plasmid pPERK_{wt}rescue-BFP (first row, Fig. 5E) or pPERK_{KD}rescue-BFP (second row, Fig. 5E). The LPA-dependent fluorescent recovery of 5'Calr-MyrCherry-3'Calr in axons of the shPERK transfected neurons was restored with co-expression of PERK_{wt}rescue-BFP but not PERK_{KD}rescue-BFP (Fig. 5E–F). Considering that PERK inhibition diminishes the injury-induced axonal Calreticulin translation (Fig. 3C and 3D), and that LPA induced translation of Calreticulin is mediated by eIF2 α phosphorylation (Vuppalanchi et al., 2012), these results together suggest that PERK-dependent eIF2 α phosphorylation selectively converges to regulate axonal Calreticulin translation.

Phosphorylated eIF2 α regulates translation of Calreticulin mRNA in axons through concerted roles of its 5'UTR and 3'UTR elements

Previous studies have shown that the *Calr* 5'UTR confers translational control in response to LPA treatment through a mechanism that requires eIF2 α phosphorylation (Vuppalanchi et al., 2012). Although the mechanism underlying this translational regulation was not described, the 5'UTR of Calreticulin mRNA cannot internally initiate translation in the axonal compartment (Pacheco and Twiss, 2012). Considering that both axotomy and LPA treatment trigger axonal Calreticulin translation (Fig. 3A and 3B) (Vuppalanchi et al., 2012), we used LPA as a translation-inducing stimulus to examine the contributions of Calr's UTR elements in eIF2 α phosphorylation-dependent translation.

To test the possibility that Calr 3'UTR impacts Calreticulin translational regulation in axons of neurons under LPA treatment, we compared FRAP signals for 5'Calr-MyrGFP-3'Calr to a reporter carrying the Calr 5'UTR and the 3'UTR of Hmgb1 (5'Calr-MyrGFP-3'Hmgb1). Dissociated rat DRG neurons expressing 5'Calr-MyrGFP-3'Calr vs. 5'Calr-MyrGFP-3'Hmgb1 mRNA sequences were subjected to FRAP following treatment with LPA. The 5'Calr-MyrGFP-3'Calr expressing DRG neurons showed robust recovery, reaching statistical significance within 6 min post-bleach that was prevented by treatment with anisomycin (Ani), a protein synthesis inhibitor (Fig. 6A–B). In contrast, neurons expressing 5'Calr-MyrGFP-3'Hmgb1 did not show significant recovery of the fluorescence signal after photobleaching (Fig. 6A–B). These data suggest that both 5' and 3'UTR of Calreticulin mRNA are needed for upregulation of Calreticulin translation in response to LPA. Thus, eIF2 α phosphorylation could be a common signaling mechanism mediating axonal Calreticulin translational in response to injury or LPA treatment.

The 3'UTR of Calreticulin mRNA contains two separate sequences that are the minimum sequences sufficient to drive axonal localization. mRNAs engineered to have a 3'UTR containing only the proximal sequence spanning from nt 1315–1412 or only the sequence spanning from 1675–1780 nt (highlighted in yellow on figure 5D) both localize to axons (Vuppalanchi et al., 2010). The nt 1315–1412 sequence (proximal element) confers ligand-dependent localization into sensory axons in response to NT3 or MAG stimulation, while the sequence from nt 1413–1780 (distal element) showed constitutive localization into sensory axons (Vuppalanchi et al., 2010). We asked whether these two elements of the Calr 3'UTR may differentially impact the LPA-induced translation of axonal Calreticulin mRNA

observed in figure 6B. For this, we generated reporters with Calr 5'UTR and 3'UTR containing only the proximal element (nt 1315–1412; referred to as 5' Calr-MyrGFP-3' Calr_{1325–1412}) or the distal element (nt 1413–1780; referred to as 5' Calr-MyrGFP-3' Calr_{1413–1780}) and used these for FRAP analyses in DRG neurons exposed to LPA (Fig. 6C–D). Distal axons of neurons expressing 5' Calr-MyrGFP-3' Calr_{1315–1412} showed significant recovery from photobleaching that was translation dependent (Fig. 6C–D). In contrast, recovery for 5' Calr-MyrGFP-3' Calr_{1413–1780} in response to LPA was overall comparable to the translation inhibited by anisomycin of 5' Calr-MyrGFP-3' Calr_{1315–1412} after LPA treatment (Fig. 6C–D). The overall levels of basal axonal translation of 5' Calr-MyrGFP-3' Calr_{1413–1780} without LPA was comparable to 5' Calr-MyrGFP-3' Calr_{1315–1412} and to the reporter with full Calr 3'UTR (supplemental figure 2). These data indicate that Calr 3'UTR proximal element (nt 1315–1412) is essential for the LPA-dependent axonal translation of Calreticulin mRNA.

Since LPA increases the phosphorylation of eIF2 α (Vuppalanchi et al., 2012), we asked if axonal translation of 5' Calr-MyrGFP-3' Calr_{1315–1412} responds to manipulation of eIF2 α phosphorylation in the absence of LPA signaling. For this, we cotransfected neurons with 5' Calr-MyrGFP-3' Calr_{1315–1412} plus a phosphomimetic construct of eIF2 α (Ser 51 to Asp mutation; eIF2 α .S51D-ECFP) (Kaufman et al., 1989) or a non-phosphorylatable eIF2 α (Ser 51 to Ala mutation; eIF2 α .S51A-ECFP) (Pathak et al., 1988). For detection, both constructs encoded an in frame ECFP fused to the C-terminus of eIF2 α .S51D or eIF2 α .S51A. By FRAP analyses, DRG neurons co-expressing the phosphomimetic eIF2 α showed robust recovery of 5' Calr-MyrGFP-3' Calr_{1315–1412} fluorescence compared to those expressing eIF2 α .S51A (Fig. 6E–F). In contrast, neurons expressing eIF2 α .S51D showed much lower fluorescence recovery of the constructs lacking the proximal element nt 1315–1412 (5' Calr-MyrGFP-3' Calr_{1413–1780}) in comparison to the fluorescence recovery of 5' Calr-MyrGFP-3' Calr_{1315–1412} (Fig. 6E–F). The recovery of 5' Calr-MyrGFP-3' Calr_{1413–1780} + eIF2 α .S51D was slightly increased compared to 5' Calr-MyrGFP-3' Calr_{1413–1780} + eIF2 α .S51A at later time points in the FRAP analysis (see analysis in legend of figure 6). In neurons expressing eIF2 α .S51A, the baseline fluorescence recovery of 5' Calr-MyrGFP-3' Calr_{1413–1780} was overall comparable to axonal fluorescence recovery of 5' Calr-MyrGFP-3' Calr_{1315–1412} in agreement with the results shown in supplemental figure 2. Taken together, these data indicate that LPA-induced eIF2 α phosphorylation specifically upregulates translation of axonal Calreticulin mRNA through a mechanism requiring both the 5'UTR and specific 3'UTR element within nt 1315–1412.

Axonal Calreticulin translation attenuates retraction of injured axons and promotes regeneration.

Since both *in vivo* and *in vitro* axotomy rapidly increased axonal Calreticulin levels, and *in vitro* this was mediated through PERK phospho-eIF2 α -dependent translation, we asked what the functional significance of this increase in axonal Calreticulin protein serves for the retraction and regenerative responses of injured axons. For this, dissociated adult rat L4–5 DRG neurons were cultured for 24 h at low density such that individual axons could be severed with a pulled glass micropipette as described above (representative inset panel on Fig. 7A). By measuring the movement of the axon tip relative to the cut site, we quantified

the extent of retraction and regeneration of the distal end of the severed axon, maintaining continuity with the cell body, over a 2 h time-lapse imaging experiment. Using this approach, we assessed the role of PERK to eIF2 α phosphorylation and subsequent translation of Calreticulin in individual injured axons. Axons in DRG cultures where PERK was inhibited using GSK2606414 (90 μ m) (Axten et al., 2012) showed significantly greater axon retraction following the axotomy compared with the control axons treated with DMSO (Fig. 7A–B and supplemental videos 1 and 2).

After PERK-eIF2 α phosphorylation, phospho-eIF2 α (eIF2 α -pS51) inhibits the guanine exchange factor activity of eIF2B complex, disabling ternary complex formation (eIF2-GTP-Met-tRNA) and limiting cap-dependent translation initiation (Kimball, 1999). ISRIB prevents the interaction of eIF2B with phospho-eIF2 α , and therefore can reverse the inhibitory effect of eIF2 α phosphorylation on general cap-dependent translation (Sekine et al., 2015). Severed axons of DRG cultures treated with ISRIB (300 nM) showed a significant increased retraction above the vehicle treated control (Fig. 7C–D). The retraction of ISRIB treated axons was similar to the axons treated with PERK inhibitor (Fig. 7E). Thus, ISRIB treatment did not rescue the axonal behavior in the first 2h after injury suggesting that not only eIF2 α phosphorylation but also the inhibition of the general cap-dependent translation could be required in the early response to injury. Interestingly, DRG neurons treated with ISRIB did not show and increase in axonal Calreticulin levels after injury compared to the control neurons (supplemental figure 3), suggesting that inhibition of general cap-dependent translation through eIF2 α phosphorylation may be necessary to activate the translation of specific mRNAs involved in the early response to axonal injury of sensory neurons. Together, these data suggest that translation of Calreticulin in axons may attenuate axon retraction after injury, thereby allowing regeneration to ensue quicker or at all.

To test the possibility that axonal translation of Calreticulin is needed for regeneration, we used shRNA (pSUPER-shRNACAL-GFP) to target rat Calreticulin (NM_022399.2) and we generated shRNA rescue constructs for Calreticulin that encoded an in frame N-terminal mCherry with the coding sequence of rat Calreticulin engineered to be resistant to the siRNA target sequence (pmCherry-CalrRescue). Determination of siRNA mediated endogenous Calreticulin knockdown was performed through western blot of lysates collected 48 h after transfection of F11 cells with pSUPERshRNA-Calr-GFP (Fig. 8A). The expression of shRNA-Calr knocked down the endogenous Calreticulin (compare lane 3 with lanes 1 and 2). Western blot of lysates from pSUPERshRNA-Calr-GFP transfected HEK 293 cells show that the shRNA effectively knocked down Calreticulin protein expression from the construct expressing rat Calreticulin sequence, pmCherry-Calr (Fig. 8B, compare lane 2 with 1 and 3). Calreticulin levels were rescued by co-transfecting the cells with pSUPERshRNA-Calr-GFP and pmCherry-CalrRescue (Fig. 8B, compare lane 5 with lane 2 and 4). In order to analyze the effect of Calreticulin knockdown in axonal outgrowth, growth of DRG neurites was measured in cultures of adult rat L4–6 DRG neurons after transfection with pSUPERshRNA-Calr-GFP or co-transfection with pSUPERshRNA-Calr-GFP plus pmcherry-CalrRescue. The expression of shRNA-Calr in DRG neurons was determined by the presence of GFP expression and the expression of pmcherry-CalrRescue was determined by the presence of mcherry expression (Fig. 8C). Interestingly, the expression of Calreticulin

shRNA in the DRG neurons significantly decreased axon lengths measured at 48 h of transfection (Fig. 8D). However, axonal length was restored to levels seen with control shRNA transfection (pSUPERshRNA-nontarget-GFP) for DRG neurons co-transfected with pSUPERshRNA-Calr-GFP and pmcherry-CalrRescue (Fig. 8D). These data suggest that Calreticulin protein supports axon growth.

We next used the *in vitro* axotomy model used in Fig. 7 to test for functional roles for Calreticulin protein in axotomy induced axon retraction. Similar to the observed effect of PERK inhibition in the response to axotomy (Fig. 7A–B), shRNA-based depletion of endogenous Calreticulin significantly increased axon retraction of the proximal cut axon end remaining attached to the soma (Fig. 8E and supplemental videos 3a–b and 4). In contrast, neurons co-transfected with shRNA-Calr plus the Calreticulin rescue construct showed minimal retraction (Fig. 8E). Indeed, expression of the rescue construct resulted in decreased retraction relative to the non-targeting shRNA and the axons underwent slight increases in length toward the site of severing (Fig. 8E). These data indicate that Calreticulin protein attenuates axon retraction after injury thereby allowing regeneration.

To address if axonal exogenous enrichment of Calreticulin would improve the basal regeneration capability of DRG neurons, we developed plasmids encoding an in frame GFP fused to the N-terminus of the rat Calreticulin sequence (NM_022399.2) followed by one of two different 3' UTR sequences at the C-terminus of the coding sequence. The 3'UTR of ACTG1 sequence restricts the mRNA into the soma (pGFP-Calr-3'ACTG1), while the 3'UTR of Actb (pGFP-Calr-3'Actb) localizes the mRNA into the axon (Bassell et al., 1998; Donnelly et al., 2011; Zheng et al., 2001). As the goal of this approach is to overexpress Calreticulin independent of any specific regulatory mechanism driven by the Calr 5'UTR, the 5'UTR was omitted and translation of the GFP-Calr was controlled constitutively by an ATG initiation codon within a proper initiation of translation sequence (Kozak, 1987). Thus, by using these subcellular differentially targeted 3'UTR constructs we aimed at increasing Calreticulin protein levels mostly in the soma or in the axon. Adult rat DRG neurons expressing GFP-Calr-3'ACTG1 or GFP-Calr-3'Actb were subjected to axotomy using a pulled glass electrode as described above and then imaged over time to evaluate the axonal response. In contrast to the effects seen with PERK inhibition and Calreticulin knockdown (Fig. 7A–B and Fig. 8E), neurons overexpressing the axonally targeted Calreticulin mRNA (GFP-Calr-3'Actb) showed no retraction and significant increased elongation over the course of the time lapse imaging compared to neurons overexpressing the GFP control and to the neurons overexpressing the soma-restricted Calreticulin (GFP-Calr-3'ACTG1) (Fig. 8F and supplemental videos 5 and 6). Moreover, the axonal behavior of DRG neurons expressing GFP-Calr-3'ACTG1 was comparable to GFP control neurons (Fig. 8F). Taken together with the increased axonal retraction seen with depletion of Calreticulin and evidence for axotomy-induced translation of Calreticulin mRNA at terminal axon cut sites, these data indicate that localized translation of Calreticulin mRNA in injured axons reduces retraction of cut axons and facilitates axon regeneration.

Discussion

In highly polarized cells, transporting proteins over long distances can take a time longer than the protein half-life (Campenot and Eng, 2000). Neurons can spatially and temporally regulate protein composition of subcellular domains through translation of mRNAs transported to these sites. For example, translational control of localized mRNAs contributes to axonal responses to guidance cues and injury (Donnelly et al., 2010). Most known mRNA regulatory elements are situated in the 5' and 3' of the UTRs. These elements act as structural platforms for the assembly of proteins generating ribonucleoparticles that will control mRNA localization (Andreassi and Riccio, 2009) and translation (Kapur et al., 2017). In the past decades, it has been shown that the 5'UTR is primarily involved in controlling mRNA translation (Lacerda et al., 2017) and the 3'UTR regulates multiple aspects of mRNA metabolism (Moore, 2005). In general, protein synthesis can be regulated globally during stress by modulating the activity of the translation initiation factor (eIFs) (Spriggs et al., 2010), at the level of individual mRNAs through sequestration from the translational machinery (Huttelmaier et al., 2005) or activating cap-independent translation mechanism at the 5'UTR sequences (Choi et al., 2018; Fernandez et al., 2002). In neurons, the 3'UTRs of localizing mRNAs frequently contain sequence elements responsible for their transport to subcellular domains (Tushev et al., 2018; Vuppalanchi et al., 2009). Calreticulin mRNA translation is regulated through the 5'UTR element by LPA-dependent phosphorylation of axonal eIF2 α (Vuppalanchi et al., 2012). This translational stimulation occurs in the axon but not cell body of sensory neurons and it is independent of any alterations in transport of Calreticulin mRNA into the axons (Vuppalanchi et al., 2012). Here we have shown that the activation of axonal Calreticulin translation in response to eIF2 α phosphorylation requires coordinated actions of both 5'UTR and 3'UTR elements of Calreticulin mRNA.

A decrease in ER Ca²⁺ perturbs protein folding in the ER activating PERK (Harding et al., 2002) that subsequently phosphorylates and inactivates eIF2 α (Harding et al., 1999; Raven and Koromilas, 2008) decreasing global cap-dependent initiation of translation (Hinnebusch and Natarajan, 2002). However, mRNAs encoding the ER chaperone proteins show a paradoxical increase in their expression despite elevation of eIF2 α PS51 during ER stress (Brostrom and Brostrom, 2003). Thus, eIF2 α phosphorylation is important in the downregulation of bulk translation under a wide variety of conditions but is also important in allowing the enhanced translation of specific mRNAs (Bellato and Hajj, 2016; Moon et al., 2018). Our findings in sensory neurons reveal that injury-induced eIF2 α phosphorylation triggers axonal Calreticulin translation at early time points after injury. This is a novel example of an ER chaperone protein locally translated, through PERK-eIF2 α phosphorylation, in response to injury.

The involvement of eIF2 α phosphorylation in acute stress conditions has been previously reviewed (Bellato and Hajj, 2016; Moon et al., 2018). However, the mechanisms regulating axonal translation are not well understood. Different mechanisms for eIF2 α -independent translation are known (Holcik, 2015). Certain mRNAs are specifically translated under cellular stress using cap-independent mechanisms (Spriggs et al., 2008). Internal Ribosome Entry Site (IRES) are 5'UTR elements that can recruit the translational machinery to an

internal position bypassing the recognition of the m⁷GTP residue (or cap) at the 5' end of most mRNAs (Baird et al., 2006). We have previously shown that 5'UTR of another chaperone protein, BiP, is capable to internally initiate translation in the axons of DRG neurons but not the 5'UTR of Calreticulin mRNA (Pacheco and Twiss, 2012). Rat Calreticulin mRNA has a short 5'UTR (63 nt) that does not contain uORFs. Some mRNAs with either an extremely short or a highly complex 5'UTR use non-canonical translation initiation mechanism that direct protein synthesis under specific physiological settings (Haimov et al., 2015). Interestingly, mRNAs encoding ERtargeted proteins are released from the ER after induced-ER stress. The weak correlation between the presence of uORF elements and translational changes for these genes suggested that alternative mechanisms for initiation of translation are being used (Reid et al., 2014). Further experiments will be necessary to rule out these possibilities for Calreticulin translation. Nevertheless, our work indicates that the 5'UTR and 3'UTR proximal elements of Calreticulin mRNA are both necessary to activate axonal protein synthesis in response to PERK-eIF2 α phosphorylation after axotomy and during acute LPA treatment. Gene-specific translational control by interactions between 5' and 3'UTR sequences have been described in bacteria (Franch et al., 1997) and RNA viruses ((Edgil and Harris, 2006). In eukaryotic RNAs, translation of human p53 mRNA is regulated by base-pairing interactions between 5' and 3'UTR sequences (Chen and Kastan, 2010).

Transected axons undergo a series of processes involving retraction, terminal enlargement formation, growth cone re-formation and axon extension that requires a dynamic protein turnover. The regeneration capability of an injured axon is dependent on the type of neuron, the age (Chierzi et al., 2005) as well as their capacity to locally synthesize new proteins and degrade others at the injury site autonomously from the cell body (Gumy et al., 2010). In this study, we analyzed the retraction and elongation of single axons of DRG neurons during the first 2h after injury. In acute stress conditions as ischemia, PERK induced P-eIF2 α -mediated translational repression is a fundamental stress response (Kumar et al., 2001; Owen et al., 2005). However, prior contradictory results found either a detrimental or beneficial value for eIF2 α phosphorylation after axonal injury (reviewed in (Bellato and Hajj, 2016)), leaving the understanding of eIF2 α signaling quite unclear. In this work, we have shown that PERK-eIF2 α phosphorylation counter the retraction of axons after axotomy. We observed that inhibition of PERK dramatically increase the axonal retraction right after injury impeding regeneration. ISRIB is an eIF2B activator that reverses the eIF2 α phosphorylation inhibitory effect in the cap-dependent mRNA translation without preventing eIF2 α phosphorylation (Sekine et al., 2015). Interestingly, the axons of DRG neurons treated with either drug, ISRIB or PERK inhibitor, retracted similarly after injury. Moreover, following axotomy the axonal Calreticulin levels of DRG neurons treated with ISRIB remained in a similar level than the uninjured axons. Therefore, not only eIF2 α phosphorylation but also inhibition of cap-dependent translation seems to be required for the translation of specific mRNAs involved in the early regenerative response of PNS axons. Thus, our data suggests that the expression of an ER stress sensors as Calreticulin, is tightly regulated during axonal injury through the inhibition of cap-dependent initiation of translation. Similarly than the mechanism described during memory formation (Chesnokova et al., 2017), eIF2 α phosphorylation and inhibition of cap-dependent translation could be a

common signaling mechanism to switch the translation machinery to specific mRNA that need to be expressed in response to injury.

ER is a major intracellular calcium store and is contained in distal axon segments of polarized neurons (Gonzalez and Couve, 2014). The release of Ca^{2+} from ER contributes significantly to the intra-axonal Ca^{2+} influx after injury (Li et al., 2013) that is necessary to promote axonal regeneration (Kim and Jin, 2015). Thus, the Ca^{2+} homeostatic alteration that should follows after the axotomy experiments performed in this work could activate PERK resulting in a PERK induced P-eIF2 α -mediated Calreticulin translation. Calreticulin is a multifunctional Ca^{2+} -binding protein that is highly enriched within the lumen of the ER (Michalak et al., 2009) where acts as a Ca^{2+} storage protein and it also assist in the correct folding and assembly of proteins (Ellgaard and Frickel, 2003). However, Calreticulin function as calcium modulator seems to be more significant than its function as a molecular chaperone in terms of cellular viability (Michalak et al., 2009; Molinari et al., 2004). The free Ca^{2+} in the ER is a balance between Ca^{2+} release, uptake and buffering by Ca^{2+} -binding proteins as Calreticulin. Moreover, Calreticulin plays key roles in modulating the sarco/endoplasmic reticulum Ca^{2+} -ATPase activity (John et al., 1998), which is activated by a rise in cytosolic Ca^{2+} and pumps Ca^{2+} into the ER (MacLennan et al., 1997). The local Calreticulin increase after axotomy of sensory neurons could help to recover calcium homeostasis after the initial triggering of injury induced Ca^{2+} waves. Thus, the axonal retraction due to calcium-dependent cytoskeletal breakdown (Wang et al., 2012) could be reduced by Calreticulin local translation to minimize subsequent retraction and promote elongation and axonal regeneration. The efficient regeneration in *C. Elegans* axons requires Calreticulin-dependent calcium fluxes within the severed neuron (Pinan-Lucarre et al., 2012). In this work, we observed that the axons of DRG neurons with decreased levels of endogenous Calreticulin retract longer distances after axotomy and they are not able to regenerate, within the time frame of the experimental design. Furthermore, the axonal growth capacity of DRG neuron was also dependent on endogenous Calreticulin levels as reflected by shorter axon lengths in neurons with depleted Calreticulin levels. This is in agreement with previous work in PC12 where Calreticulin promotes NGF-induced neurogenesis (Cheng et al., 2015) through its Ca^{2+} -buffering domain (Shih et al., 2012). Since both PERK inhibition and Calreticulin knockdown affect the axonal response after injury in the same direction, likely the inhibition of the local increase of Calreticulin in response to injury is the cause of the lack of regenerative response. Thus, in DRG sensory neurons Calreticulin translation, through PERK-eIF2 α phosphorylation, could be tightly regulated spatially and temporally to restrict axon retraction at early time points after injury. Interestingly, axonal overexpression of Calreticulin mRNA remarkably increased the elongation capacity beyond the cut site in a short period of time after axotomy, indicating that this approach may be used to promote axon regeneration.

Conclusions

Axonal Calreticulin expression is tightly regulated during injury through the inhibition of cap-dependent initiation of translation by PERK-eIF2 α phosphorylation. This mechanism of translation requires concerted roles of Calreticulin 5'UTR and 3'UTR mRNA elements. Therefore, based in our data and supported by previous literature we suggest that the local

increase of Calreticulin translation at the injury site could contribute to calcium homeostasis regulating axonal retraction and promoting the regeneration in the PNS axons.

Materials and methods

Animal surgery.

All animal work was conducted under Institutional Animal Care and Use Committee (IACUC)-approved protocols at Drexel University and at Temple University. For nerve injury, Male Sprague Dawley rats (150–225 g) were anesthetized using isoflurane and then subjected to a unilateral conditioning sciatic nerve crush at mid-thigh level as previously described (Twiss et al., 2000) using a Dumont 0 forceps (Smith and Skene, 1997). Animals were euthanized at 1 h, 6 h, 18 h and 7 days after nerve crush and sciatic nerves (naïve and injured) were collected proximal to the crush injury site with a corresponding level of naïve nerve collection. Tissues were fixed in 4% paraformaldehyde for 2 h, cryoprotected in buffered 30% sucrose at 4°C overnight, and processed for cryostat sectioning (10 µm thick). The contralateral nerve to crush injury was exposed but not manipulated to use it as a control (i.e., naïve).

DNA expression constructs.

All DNA constructs outlined below were sequence validated before use. All the constructs used for studying axonal translation through Calreticulin UTR elements were generated in the pcDNA3.1+ backbone (Invitrogen, V79020). For these, we used eGFP and mCherry sequences with an N-terminal myristoylation signal (*MyrGFP* and *MymCherry*, respectively). Diffusion limited *MyrGFP* reporter constructs, 5'Calr-*MyrGFP*-3'Calr, 5'Calr-*Mymcherry*-3'Calr and 5'Actb-*MyrGFP*-3'Calr, were previously described (Vuppalanchi et al., 2012). The Calr 3'UTR from 5'Calr-*MyrGFP*-3'Calr was replaced NotI/XhoI with the segments corresponding to nt 1315–1412 (Calr 3'UTR proximal element) or corresponding to nt 1413–1780 (Calr 3'UTR distal element) of the rat Calreticulin mRNA (GenBank accession no. [NM_022399](#)) that were cut NotI/XhoI from the 3'UTR deletion mutants constructs previously described (Vuppalanchi et al., 2010) generating the vectors 5'Calr-*MyrGFP*-3'Calr_{1315–1412} and 5'Calr-*MyrGFP*-3'Calr_{1413–1780} respectively. The *MyrGFP* segments from 5'Calr-*MyrGFP*-3'Calr_{1315–1412} and 5'Calr-*MyrGFP*-3'Calr_{1413–1780} were replaced BamHI/NotI with the *Mymcherry* fragment from 5'Calr-*Mymcherry*-3'Calr generating the vectors 5'Calr-*Mymcherry*-3'Calr_{1312–1412} and 5'Calr-*Mymcherry*-3'Calr_{1413–1780} respectively. To generate the construct 5'Calr-*MyrGFP*-3'Hmgb1, Calr 3'UTR from 5'Calr-*MyrGFP*-3'Calr was replaced NotI/XhoI with the rat sequence of Hmgb1 3'UTR that was cut NotI/XhoI from the construct with the rat Hmgb1 3'UTR previously described (Donnelly et al., 2013).

The adenoviral vectors that express the sequences of eIF2α mutants S51D and S51A (Vuppalanchi et al., 2012) were used as PCR templates to generate the cDNAs of the eIF2α mutants S51D and S51A. The primers were engineered to include 5' HindIII and 3' BamHI restriction sites in the cDNA products. The PCR conditions were as follows: 95°C for 1 min, 58°C for 1 min, and 72°C for 1 min for 35 cycles with a final 72°C extension for 10 min. The digested PCR products were subcloned into pECFP-N1 (BD Biosciences Clontech,

#6900–1) to generate constructs encoding an in frame ECFP fused to the C-terminus of eIF2 α S51D or eIF2 α S51A (pS51D-ECFP and pS51A-ECFP respectively). The vectors that express mouse sequence of PERK_{wt} (addgene plasmid # 21814) and mouse sequence of PERK_{kinase dead} (addgene plasmid # 21815) were used as PCR templates to generate the cDNAs of PERK_{wt} and PERK_{KinaseDead}. The primers were engineered to include 5' NheI and 3' XhoI restriction sites in the cDNA products. The PCR conditions were as follows: 95°C for 1 min, 58°C for 1 min, and 72°C for 1 min for 35 cycles with a final 72°C extension for 10 min. The digested PCR products were subcloned into the pTagBFP-N vector (evrogen products, FP172) to generate constructs encoding an in frame BFP fused to the C-terminus of PERK_{wt} or PERK_{KinaseDead} (pPERK_{wt}-BFP and pPERK_{KD}-BFP respectively). Replacing K618 of PERK with alanine (K618A) abolishes the ability of the protein to undergo autophosphorylation or to phosphorylate eIF2 α (Harding et al., 1999). Both constructs encoded an in frame BFP fused to the C-terminus of PERK_{wt} (pPERK_{wt}-BFP) or and PERK_{KinaseDead} (pPERK_{KD}-BFP), respectively. For siRNA-resistant pPERK_{wt}-Rescue-BFP and pPERK_{KD}-Rescue-BFP construct, 3 nucleotides of the siRNA-targeted regions (GGTCATGGCGTTTAGTAAG) were mutated in the plasmids pPERK_{wt}-BFP and pPERK_{KD}-BFP using QuikChange XL Site-DirectedMutagenesis kit (Stratagene). The following primers were used: sense, 5'-GCTGATTGGAAGGTA*ATGGCT*TTTAGC*AGGAAGGGAGGCCG -3' and antisense, 5'-CGGCCTCCCTTCCAG*CTAAAA*GCCATT*ACCTTCCAATCAGC-3' (asterisks indicate mutated nucleotides).

Rat Calreticulin cDNA (GenBank accession no. [NM_022399](#)) was generated by RT-PCR and cloned into pTagBFP-N plasmid (evrogen products, FP172). For this, RNA (200 ng) isolated from rat DRG cultures was reverse transcribed using iScript cDNA synthesis kit (Bio-Rad). The cDNA was then amplified using Pfu DNA polymerase (Stratagene). The PCR conditions were as follows: 95°C for 1 min, 60°C for 1 min, and 72°C for 1 min for 35 cycles with a final 72°C extension for 10 min. Primers spanning the coding sequence of Calreticulin (nt 1–1251) were engineered to include 5' XhoI and 3' SacII restriction sites in the cDNA products. The purified PCR product was cloned upstream of BFP, generating pCalr-BFP. For siRNA-resistant pCalr-BFPrescue construct, 3 nucleotides of the siRNA-targeted regions (GTGCTGATCAACAAGGATA) were mutated in the plasmid pCalr-BFP using QuikChange XL Site-DirectedMutagenesis kit (Stratagene). The following primers were used: sense, 5'-CAAGGGCAAGAACGTGCTA*ATCAAT*AAGGAC*ATCCGGTGTAAGGATG-3' and antisense, 5'-CATCCTTACACCGGATG*TCCTTA*TTGATT*AGCACGTTCTTGCCCTTG-3' (asterisks indicate mutated nucleotides).

The vectors pGFP-Calr-3'Actb and pGFP-Calr-3'ACTG1 were generated as follow. 5'Calr-MyrGFP-3'Calr DNA was used as PCR template to amplify the sequence 5'HindIII-GFP-3'BamHI that was subcloned into pcDNA3.1+ backbone (Invitrogen, V79020) generating pGFP vector. Rat Calreticulin cDNA was amplified by PCR using pCalr-BFPrescue as template. The PCR conditions were as follows: 95°C for 1 min, 56°C for 1 min, and 72°C for 1 min for 35 cycles with a final 72°C extension for 10 min. Primers spanning the coding sequence of rat Calreticulin (nt 521251) were engineered to include

5'NotI and 3'XbaI restriction sites in the cDNA that was cloned in frame downstream the GFP sequence of pGFP generating pGFP-Calr. The rat sequences of 3'Actb and 3' ACTG1 UTRs were amplified by PCR using as templates previously described vectors (Willis et al., 2007). The primers were engineered with 5'XbaI and 3'ApaI restriction sites. The PCR conditions were as follows: 95°C for 1 min, 56°C for 1 min, and 72°C for 1 min for 35 cycles with a final 72°C extension for 10 min. The digested PCR products were subcloned in pGFP-Calr downstream of Calreticulin sequence generating pGFP-Calr-3'Actb or pGFP-Calr-3'ACTG1. The GFP sequence of pGFP-Calr was replaced with the mcherry sequence HindIII/NotI generating the vector pmcherry-CalrRescue. The vector pmCherry-Calr was generated as follow. Rat Calreticulin cDNA was amplified by PCR using pCalr-BFP as template. The PCR conditions were as follows: 95°C for 1 min, 56°C for 1 min, and 72°C for 1 min for 35 cycles with a final 72°C extension for 10 min. Primers spanning the coding sequence of Calreticulin (nt 52–1251) were engineered to include 5' NotI and 3' XbaI restriction sites. The PCR product was used to replace the CalrRescue sequence on pmcherry-CalrRescue generating pmcherry-Calr.

siRNA depletion of endogenous Calreticulin and PERK mRNAs.

shRNA sequences were expressed based on pSuper.puro (VEC-PBS-0007/0008, OligoEngine) with modifications. GFP sequence was subcloned PstI/NheI on the plasmid pSuper.puro generating the vector pSuper.GFP.puro. Calreticulin (pSUPERshRNA-Calr-GFP) or the PERK silencing plasmid (pSUPERshRNA-PERK-GFP) [target rat sequences GTGCTGATCAACAAGGATA (nt 525–544, GenBank accession no. [NM_022399](#)) and GGTCATGGCGTTTAGTAAG (nt 929–948, GenBank accession no. [NM_031599](#)), respectively], were generated according to the manufacturer instructions (*OligoEngine*). Both Calreticulin and PERK shRNA target sequences were obtained through screening of a list of predicted shRNA targets sequence by the online siRNA design tool siDRM (Gong et al., 2008). The control shRNA-nontarget (target sequence GCGCGATAGCGCTAATAAT) has no homology to any mammalian gene. For “rescue” experiments, dissociated DRGs were co-transfected, as explained below, with the corresponding shRNA expressing plasmid and recombinant PERK or Calreticulin expression constructs and they were cultured for 48 h before imaging. Protein depletion were quantified by immunoblot 48 h after transfection as explained below.

DRG explants culture.

Fertilized chicken eggs containing embryos of either sex were obtained from Charles River. At embryonic day 8 (E8), embryos were removed from the eggs and the DRG dissected out. Whole explants were cultured, using previously described protocols (P.I. Lelkes et al., 2006). The culturing substrata were coated with 100 µg/ml polylysine (SIGMA, P9011) in borate buffer overnight and 25 µg/ml laminin (Invitrogen) in PBS 4 h. Explants were cultured in defined F12H medium with NGF as previously described (Ketschek and Gallo, 2010) and were used for experiments 24 h after plating in video dishes that provide a fixed substratum during severing, unlike coverslips placed in dishes. Six to eight cultures, each containing 3 DRG explants, were used per group and axons were manually severed ~ 800 – 1000 µm from the soma on one side of the explants using an interchangeable blade 1.5 mm cutting edge (Fine Science Tool, 10035–05). The unsevered explants in the same cultures served as

internal controls. PERK inhibitor (GSK2606414, 90 μ M), ISRIB (SML-0843, 300 nM) or DMSO was added 15 min before severing the axons. The cultures were immunostained 20 min after axotomy.

Cell culture and transfections.

HEK 293 cells, were maintained in 10% fetal bovine serum supplemented DMEM at 37 °C and 5% CO₂ on plastic dishes. Neuronal-like F11 cells, a hybridoma of embryonic rat DRG neurons and mouse neuroblastoma cell line N18TG (Platika et al., 1985), were cultured in DMEM:F12, 10% fetal bovine serum, 100 U/ml penicillin, and 0.1 mg/ml streptomycin (Sigma) at 37 °C and 5% CO₂ on plastic dishes. HEK-293 and F11 cells were transfected with 2 mg plasmid using Lipofectamine 2000 Reagent per manufacturer's instructions (Invitrogen, 11668–027). Transfected cells were cultured for 48 h before lysates collection.

Primary cultures of dorsal root ganglion (DRG) were prepared from adult Sprague Dawley rats (175 g). These were dissociated using 5 units/ μ l collagenase type XI (Sigma, C9697) for 30 min. The dissociated DRGs were transfected using *AMAXA Nucleofector* apparatus with the SCN Nucleofector kit (program G-8; Lonza, Inc.) and resuspended in DMEM/F12 (Corning, 16–405-CV) with 10% horse serum (Hyclone) and cultured for 48h. The culture media was replaced at 20 h post-transfection with media containing 10 mM arabinofuranosyl cytidine (SIGMA-Aldrich, C6645) to decrease proliferation of non-neuronal cells. Dissociated DRG neurons were plated in videodishes coated with 100 μ g/ml polylysine (SIGMA, P9011) in H₂O for 1 h and 25 μ g/ml laminin (Invitrogen) in PBS overnight. DRG neurons were plated in videodishes for 24 h in the experimental groups of DRG neurons treated with drugs (PERK inhibitor and ISRIB), or for 48 h in the transfected neurons studies, before axotomy and live imaging analysis. DRG neurons that were subject to axonal growth analysis were plated on coated coverslips and fixed 48 h after transfection using 8% paraformaldehyde (PFA) containing 5% sucrose for 15 min, washed in PBS, washed in deionized water, and mounted in no-fade mounting medium. The samples were imaged using a Zeiss 200 M microscope equipped with an Orca-ER camera (Hamamatsu) in series with a PC workstation running Axiovision software for image acquisition and analysis. Imaging was performed using a Zeiss Plan-Neofluar 20X objective (0.5 NA), 2X2 camera binning, minimal light exposure. Acquisition parameters were set to prevent saturation of the signal in axons

Immunocytochemistry and quantification of fluorescence intensities.

Cultures of chicken DRG explants were fixed, 20 min after severing the axons, using 8% paraformaldehyde (PFA) containing 5% sucrose for 15 min; Samples were then blocked using 10% goat serum in PBS with 0.1% Triton X-100 (GST) and stained with primary antibodies for 60 min, washed in PBS, incubated with secondary antibodies for 60 min (Alexa 488, 1:400, Invitrogen), washed in PBS, washed in deionized water, and mounted in no-fade mounting medium as previously described (Gallo and Letourneau, 1999). The following primary antibodies were used in conjunctions with the described fixation protocol above and at the described dilutions: P-eIF2 α (1:100; Cell Signaling, #9721), P-PERK (Thr980) (1:1000, cell signaling, #3179S) and Calreticulin (1:100; abcam, ab2907). For quantification of the levels of immunolabeled axonal proteins, samples were visualized

using a Zeiss 200 M microscope equipped as described above using a Zeiss Plan-Apochromat 40X objective (1.0 NA). Phase contrast images of the axons acquired at the same times as the GFP channel were used to determine the location of the axon. Camera binning of 2X2 was used and the acquisition parameters were set so that the entire dataset was within the dynamic range of measurement. A minimum of 40 axons was scored per culture in the peripheral halo of both severing axons and control axons (no severing axons). Only distal axons that were not contacting other axons were scored. The distal 30–50 μm from the tip of severed axon shaft remaining attached to the soma was defined as a region of interest using the Zeiss Axiovision software interactive measurement module, and the area of the region of interest was multiplied by the background subtracted mean intensity of the stain to obtain the total integrated staining intensity within the region of interest.

For sciatic nerve tissue sections, immunofluorescence was performed as previously published (Merianda et al., 2013). Tissue sections were equilibrated in PBS and then incubated in 20 mM Glycine for 10 minutes each with three changes followed by 0.25 M NaBH₄ for 30 min to quench auto-fluorescence. Permeabilized with 0.2 % Triton X-100 for 15 min and incubated in blocking buffer for an hour at room temperature (Vuppalanchi et al., 2010). Tissues were incubated in primary antibodies overnight at 4 C. The primary antibodies used were rabbit anti-Calreticulin (1:100; Stressgen), chicken anti-neurofilament Heavy NF H (1:800; Millipore), chicken anti-NF Light (1:400; Aves) and chicken anti-NF Medium (1:200; Aves). After several washes with PBS, samples were incubated with secondary antibodies for 1 h at room temperature. Secondary antibodies used were Alexa 488 conjugated anti-chicken (1:400; Invitrogen) and Alexa 555 conjugated anti-rabbit (1:500; Invitrogen). After series of washes in PBS, samples were mounted on Prolong Gold Antifade with DAPI (Invitrogen). Tissue sections were imaged using Zeiss LSM 700 laser scanning confocal microscope. All images were matched for acquisition parameters and post-processing. Calreticulin protein intensity was calculated from images that were matched for exposure time, gain, offset, and post-processing parameters. NF signals were used to trace axons. *Image J* was then used to calculate the average pixels/ μm^2 in these areas for >25 axons as described (Merianda et al., 2013; Vuppalanchi et al., 2012).

Fluorescence recovery after photobleach.

To monitor localized translation of diffusion-limited *MyrGFP* or *Mymcherry* reporters, we used fluorescence recovery after photobleaching (FRAP) as previously described (Yudin et al., 2008) with minor modifications. Briefly, transfected DRG cultures were analyzed 48 h after transfection for intra-axonal GFP or mcherry fluorescence using Zeiss LSM700 confocal microscope fitted with an environmental chamber to maintain 5% CO₂ and 37 C over the duration of the imaging sequences. 40X C-Apochromat-Korr M27 water immersion objective (1.20 NA) was used for imaging, and the confocal pinhole was set to 4 airy units to ensure that the entire 2–4 μm thickness of axons was fully photobleached. DIC imaging was used to visualize neuronal processes; these are easily distinguished from Schwann cells in these cultures by presence of a terminal growth cone and length of several hundred microns. This was facilitated by the use of low-density cultures for these imaging studies. Prior to photobleaching, neurons were imaged every 60 sec for 2 min to establish baseline intensity using 488 and 555 nm lasers at 6.0 and 0.5% power, respectively. For photobleaching, the

terminal 150 μm of distal axon was exposed to 100% laser power at 488 and/or 555 nm (for GFP and mCherry, respectively) to reach a pixel intensity of <5% of the prebleach signals (50 iterations). Recovery of *Myr*mCherry and *Myr*GFP was then monitored in a region of interest (ROI) comprising the terminal 50 μm of the axons every 60 sec. over 28 min. using 488 nm laser at 0.5% power and 555 nm laser at 6.0% power. To test for translation-dependent recovery, cultures were pretreated with 150 μM anisomycin (A9789, SIGMA-Aldrich) for 30 min or with 150 $\mu\text{g}/\text{ml}$ cycloheximide (01810, SIGMA-Aldrich) prior to photobleaching as previously described (Pacheco and Twiss, 2012). Transfected DRG cultures were imaged 1 h after exposure to 30 μM LPA (BioMol). Images were analyzed using ZEN 2010 software package (Zeiss) to calculate the mean fluorescence intensity within the ROI. Fluorescent intensity at each time point was normalized to the average pre-bleach intensity. Each construct was analyzed in 8 neurons over at least 4 independent transfections/culture preparations.

To monitor localized translation of diffusion-limited *Myr*GFP reporter in response to injury of DRG neurons, we used FRAP analysis with measurements in the cut end of the distal shaft of axons attached to the soma 20 min after axotomy. Briefly, DRG cultures were analyzed 48 h after transfection for intra-axonal GFP fluorescence using a Zeiss Axiovert 200 M microscope equipped with an Orca-ER camera (Hamamatsu) in series with a PC workstation running Axiovision software for image acquisition and analysis. Cultures were placed on a heated microscope stage (Zeiss temperable insert P with objective heater) for 15 min before imaging. Imaging was performed using a Zeiss Pan-Neofluar 100X objective (1.3 NA), 2X2 camera binning, minimal light exposure. Acquisition parameters were set to prevent saturation of the signal in axons. The FRAP assays were started 20 min after axotomy. Frames were acquired just before and immediately after bleaching and at 5 min intervals thereafter over 35 min time-lapse experiments. Photobleaching of *Myr*GFP was performed in the terminal 60–80 μm of distal axon remained attached to the soma, by using 30–45 s exposure in the entire imaging field to light from a 100 W source. Phase contrast images of the axons acquired at the same times as the GFP channel were used to determine the location of the axon at early time points in the FRAP when the GFP signal is otherwise too low to detect the axon. Only axons that were photobleached by 90% of their initial value were used in the analysis. To track recovery, the mean background subtracted intensity of GFP was measured in a fixed ROI at the terminal axon using the Zeiss Axiovision software interactive measurement module to calculate the mean fluorescence intensity within the ROI.

Live imaging analysis of axonal growth after axotomy.

DRG dissociated cultured were grown 24 h (drugs experiments) or 48 h (transfections experiments) and a single axon per DRG neuron was severed under phase-contrast with a pulled glass electrode set up in a manual micromanipulator (WPI, M3301R). The position of axotomy was set up in the distal axon close to the axonal tip (50–100 μm from the end of the axon) and the position and appearance of the axons was recorded before and after the lesion. We monitored regeneration by imaging the movement of the axons from the lesion site right after cut by time-lapse microscopy every 5 min during 2h time-lapse imaging experiment. The analysis was performed under phasecontract on a Zeiss Axio Observer Z1 inverted microscope, in series with a PC workstation running Axiovision software for image

acquisition and analysis. Cultures were placed on a heated microscope stage (Zeiss temperable insert P S1 with objective heater 2000) associated to a temperature control module (TEMPCONTROLLER 2000–2, PECON). PERK inhibitor (GSK2606414, 90 μ M) and ISRIB (SML-0843, SIGMA, 300 nM) drugs were added to the cultures 10–15 min before severing the axons. The site of axotomy was set up as zero μ m and the axonal movement was quantified using Image J software (NIH) by tracing from the axon tip the axonal length changes between time frames acquisitions. The values were represented every 5 min along the 2h time-lapse imaging experiment as the position of the axons at each time point respect the cut site (X axis). Negative values represent axonal positions retracted from the lesion site and positive values represent axonal positions elongated beyond the cut site.

Immunoblotting.

For detection of endogenous PERK and Calreticulin knockdown, F11 cells were lysed 48h after transfection in RIPA buffer at 4 °C for 20 min. Lysates were cleared by centrifugation at 13,000 \times g, 4 °C; cleared lysates were normalized for protein concentration by Bradford assay and then processed for SDS/PAGE. Fractionated proteins were transferred to PVDF membranes, blocked for non-specific binding using 5% non-fat dry milk in Tris-buffered saline (TBS) and then probed with anti-eIF2 α (1:1000, cell signaling, #9722S) or anti-PERK (1:1000, cell signaling, #3192S) overnight at 4 °C in blocking buffer. After washing in TBS, blots were incubated in HRP-conjugated anti-rabbit secondary antibodies (1:10,000; Cell Signaling, #7074) and developed with ECL^{Plus} (Amersham). For detection of recombinants PERK (PERK-BFP) and Calreticulin (mcherry-Calr) recombinant proteins, HEK-293 cells were lysed 48h after transfection in RIPA buffer at 4°C for 20 min following the same immunoblotting protocol explained above and then probed with anti-RFP (1:1000, Allele, ABP-MAB-RT008) overnight at 4°C in blocking buffer. After washing in TBS, blots were incubated in HRP-conjugated anti-mouse secondary antibodies (1:10,000; Cell Signaling, #7076) and developed with ECL^{Plus} (Amersham). β -Actin Antibody (C4) (sc-4778, Santa Cruz) was used as a loading control.

Statistical analyses.

The GraphPad Prism 5 software package (La Jolla, CA) was used for all statistical analyses. Student's *t* test was used to compare two means of independent groups. These included the data from axonal length measurements in the static imaging experiments as well as from quantified immunofluorescence signals from sciatic nerve sections and chicken explants experiments. Data generated from live imaging experiments as FRAP studies, were statistically tested by two-way ANOVA with Bonferroni *post hoc* test multiple comparisons to compare fluorescence signal intensities at different time points as previously published (Pacheco and Twiss, 2012; Vuppalachchi et al., 2010); time-lapse imaging to study axonal regeneration after axotomy was statistically tested by regression analysis. All values were expressed as mean \pm standard error of the mean (SEM). P values of ≤ 0.05 were considered as significant.

Supplementary Material

Refer to Web version on PubMed Central for supplementary material.

Acknowledgments

We are thankful to Martinez-Salas E for sharing the plasmid pSuper.puro. This work was supported by the National Institutes of Health (NS078030 to GG).

The abbreviations used are:

PNS	peripheral nervous system
CNS	central nervous system
Calr	Calreticulin; Actb, β -actin
ACTG1	γ -actin; Hmgb1, amphoterin
UTR	untranslated region
uORF	upstream open reading frame
IRES	internal ribosome entry site
eIF	eukaryotic initiation factor
Myr	myristoylation element
GFP	green fluorescent protein
DAPI	4',6-diamidino-2-phenylindole
DRG	dorsal root ganglion
HEK	human embryonic kidney cells
Ca²⁺	Calcium
ER	endoplasmic reticulum
PERK	(PKR)-like ER kinase
LPA	lysophosphatidic acid
ISRIB	integrated stress response inhibitor
NF	neurofilament
NGF	nerve growth factor
NT3	neurotrophin 3
MAG	myelin-associated glycoprotein
PBS	phosphate-buffered saline
ROI	region of interest
FRAP	fluorescent recovery after photobleaching

RT	reverse transcriptase-coupled PCR
ANOVA	analysis of variance

References

- Aakalu G, Smith WB, Nguyen N, Jiang C, Schuman EM, 2001 Dynamic visualization of local protein synthesis in hippocampal neurons. *Neuron* 30, 489–502. [PubMed: 11395009]
- Andreassi C, Riccio A, 2009 To localize or not to localize: mRNA fate is in 3'UTR ends. *Trends Cell Biol* 19, 465–474. 10.1016/j.tcb.2009.06.001. [PubMed: 19716303]
- Axten JM, Medina JR, Feng Y, Shu A, Romeril SP, Grant SW, Li WH, Heerding DA, Minthorn E, Mencken T, Atkins C, Liu Q, Rabindran S, Kumar R, Hong X, Goetz A, Stanley T, Taylor JD, Sigethy SD, Tomberlin GH, Hassell AM, Kahler KM, Shewchuk LM, Gampe RT, 2012 Discovery of 7-methyl-5-(1-([3-(trifluoromethyl)phenyl]acetyl)-2,3-dihydro-1H-indol-5-yl)-7H-pyrrolo[2,3-d]pyrimidin-4-amine (GSK2606414), a potent and selective first-in-class inhibitor of protein kinase R (PKR)-like endoplasmic reticulum kinase (PERK). *J Med Chem* 55, 7193–7207. 10.1021/jm300713s. [PubMed: 22827572]
- Baird SD, Turcotte M, Korneluk RG, Holcik M, 2006 Searching for IRES. *Rna* 12, 1755–1785. 10.1261/rna.157806. [PubMed: 16957278]
- Bassell GJ, Zhang H, Byrd AL, Femino AM, Singer RH, Taneja KL, Lifshitz LM, Herman IM, Kosik KS, 1998 Sorting of beta-actin mRNA and protein to neurites and growth cones in culture. *The Journal of neuroscience : the official journal of the Society for Neuroscience* 18, 251–265. [PubMed: 9412505]
- Bellato HM, Hajj GN, 2016 Translational control by eIF2alpha in neurons: Beyond the stress response. *Cytoskeleton (Hoboken)* 73, 551–565. 10.1002/cm.21294. [PubMed: 26994324]
- Bi J, Tsai NP, Lu HY, Loh HH, Wei LN, 2007 Copb1-facilitated axonal transport and translation of kappa opioid-receptor mRNA. *Proc Natl Acad Sci U S A* 104, 13810–13815. 10.1073/pnas.0703805104. [PubMed: 17698811]
- Bradke F, Fawcett JW, Spira ME, 2012 Assembly of a new growth cone after axotomy: the precursor to axon regeneration. *Nat Rev Neurosci* 13, 183–193. 10.1038/nrn3176. [PubMed: 22334213]
- Brostrom MA, Brostrom CO, 2003 Calcium dynamics and endoplasmic reticular function in the regulation of protein synthesis: implications for cell growth and adaptability. *Cell Calcium* 34, 345–363. [PubMed: 12909081]
- Campbell DS, Holt CE, 2001 Chemotropic responses of retinal growth cones mediated by rapid local protein synthesis and degradation. *Neuron* 32, 1013–1026. [PubMed: 11754834]
- Campanot RB, Eng H, 2000 Protein synthesis in axons and its possible functions. *J Neurocytol* 29, 793–798. [PubMed: 11466471]
- Chatterjee S, Pal JK, 2009 Role of 5'- and 3'-untranslated regions of mRNAs in human diseases. *Biol Cell* 101, 251–262. 10.1042/BC20080104. [PubMed: 19275763]
- Chen J, Kastan MB, 2010 5'-3'-UTR interactions regulate p53 mRNA translation and provide a target for modulating p53 induction after DNA damage. *Genes Dev* 24, 2146–2156. 10.1101/gad.1968910. [PubMed: 20837656]
- Cheng Y, Yang C, Zhao J, Tse HF, Rong J, 2015 Proteomic identification of calcium-binding chaperone calreticulin as a potential mediator for the neuroprotective and neurotogenic activities of fruit-derived glycoside amygdalin. *J Nutr Biochem* 26, 146–154. 10.1016/j.jnutbio.2014.09.012. [PubMed: 25465157]
- Chesnokova E, Bal N, Kolosov P, 2017 Kinases of eIF2a Switch Translation of mRNA Subset during Neuronal Plasticity. *Int J Mol Sci* 18 10.3390/ijms18102213.
- Chierzi S, Ratto GM, Verma P, Fawcett JW, 2005 The ability of axons to regenerate their growth cones depends on axonal type and age, and is regulated by calcium, cAMP and ERK. *Eur J Neurosci* 21, 2051–2062. 10.1111/j.1460-9568.2005.04066.x. [PubMed: 15869501]
- Cho Y, Cavalli V, 2014 HDAC signaling in neuronal development and axon regeneration. *Current opinion in neurobiology* 27, 118–126. 10.1016/j.conb.2014.03.008. [PubMed: 24727244]

- Choi JH, Wang W, Park D, Kim SH, Kim KT, Min KT, 2018 IRES-mediated translation of cofilin regulates axonal growth cone extension and turning. *EMBO J* 37 10.15252/embj.201695266.
- Donnelly CJ, Fainzilber M, Twiss JL, 2010 Subcellular communication through RNA transport and localized protein synthesis. *Traffic* 11, 1498–1505. 10.1111/j.1600-0854.2010.01118.x. [PubMed: 21040295]
- Donnelly CJ, Park M, Spillane M, Yoo S, Pacheco A, Gomes C, Vuppalachchi D, McDonald M, Kim HH, Merianda TT, Gallo G, Twiss JL, 2013 Axonally synthesized beta-actin and GAP-43 proteins support distinct modes of axonal growth. *The Journal of neuroscience : the official journal of the Society for Neuroscience* 33, 3311–3322. 10.1523/JNEUROSCI.1722-12.2013. [PubMed: 23426659]
- Donnelly CJ, Willis DE, Xu M, Tep C, Jiang C, Yoo S, Schanen NC, Kirn-Safran CB, van Minnen J, English A, Yoon SO, Bassell GJ, Twiss JL, 2011 Limited availability of ZBP1 restricts axonal mRNA localization and nerve regeneration capacity. *EMBO J* 30, 4665–4677. 10.1038/emboj.2011.347. [PubMed: 21964071]
- Edgil D, Harris E, 2006 End-to-end communication in the modulation of translation by mammalian RNA viruses. *Virus Res* 119, 43–51. 10.1016/j.virusres.2005.10.012. [PubMed: 16307817]
- Ellgaard L, Frickel EM, 2003 Calnexin, calreticulin, and ERp57: teammates in glycoprotein folding. *Cell Biochem Biophys* 39, 223–247. 10.1385/CBB:39:3:223. [PubMed: 14716078]
- Elmes SJ, Millns PJ, Smart D, Kendall DA, Chapman V, 2004 Evidence for biological effects of exogenous LPA on rat primary afferent and spinal cord neurons. *Brain Res* 1022, 205–213. 10.1016/j.brainres.2004.07.005. [PubMed: 15353230]
- Fernandez J, Yaman I, Sarnow P, Snider MD, Hatzoglou M, 2002 Regulation of internal ribosomal entry site-mediated translation by phosphorylation of the translation initiation factor eIF2alpha. *The Journal of biological chemistry* 277, 19198–19205. 10.1074/jbc.M201052200. [PubMed: 11877448]
- Franch T, Gulyaev AP, Gerdes K, 1997 Programmed cell death by hok/sok of plasmid R1: processing at the hok mRNA 3'-end triggers structural rearrangements that allow translation and antisense RNA binding. *J Mol Biol* 273, 38–51. 10.1006/jmbi.1997.1294. [PubMed: 9367744]
- Gallo G, Letourneau PC, 1999 Different contributions of microtubule dynamics and transport to the growth of axons and collateral sprouts. *The Journal of neuroscience : the official journal of the Society for Neuroscience* 19, 3860–3873. [PubMed: 10234018]
- Gong W, Ren Y, Zhou H, Wang Y, Kang S, Li T, 2008 siDRM: an effective and generally applicable online siRNA design tool. *Bioinformatics* 24, 2405–2406. 10.1093/bioinformatics/btn442. [PubMed: 18718944]
- Gonzalez C, Couve A, 2014 The axonal endoplasmic reticulum and protein trafficking: Cellular bootlegging south of the soma. *Semin Cell Dev Biol* 27, 23–31. 10.1016/j.semcdb.2013.12.004. [PubMed: 24361785]
- Gumy LF, Tan CL, Fawcett JW, 2010 The role of local protein synthesis and degradation in axon regeneration. *Experimental neurology* 223, 28–37. 10.1016/j.expneurol.2009.06.004. [PubMed: 19520073]
- Haimov O, Sinvani H, Dikstein R, 2015 Cap-dependent, scanning-free translation initiation mechanisms. *Biochim Biophys Acta* 1849, 1313–1318. 10.1016/j.bbagr.2015.09.006. [PubMed: 26381322]
- Hanz S, Perlson E, Willis D, Zheng JQ, Massarwa R, Huerta JJ, Koltzenburg M, Kohler M, van-Minnen J, Twiss JL, Fainzilber M, 2003 Axoplasmic importins enable retrograde injury signaling in lesioned nerve. *Neuron* 40, 1095–1104. [PubMed: 14687545]
- Harding HP, Calton M, Urano F, Novoa I, Ron D, 2002 Transcriptional and translational control in the Mammalian unfolded protein response. *Annu Rev Cell Dev Biol* 18, 575–599. 10.1146/annurev.cellbio.18.011402.160624. [PubMed: 12142265]
- Harding HP, Zhang Y, Ron D, 1999 Protein translation and folding are coupled by an endoplasmic-reticulum-resident kinase. *Nature* 397, 271–274. 10.1038/16729. [PubMed: 9930704]
- Hinnebusch AG, Natarajan K, 2002 Gcn4p, a master regulator of gene expression, is controlled at multiple levels by diverse signals of starvation and stress. *Eukaryot Cell* 1, 22–32. [PubMed: 12455968]

- Holcik M, 2015 Could the eIF2 α -Independent Translation Be the Achilles Heel of Cancer? *Front Oncol* 5, 264 10.3389/fonc.2015.00264. [PubMed: 26636041]
- Huttelmaier S, Zenklusen D, Lederer M, Dichtenberg J, Lorenz M, Meng X, Bassell GJ, Condeelis J, Singer RH, 2005 Spatial regulation of beta-actin translation by Src-dependent phosphorylation of ZBP1. *Nature* 438, 512–515. 10.1038/nature04115. [PubMed: 16306994]
- John LM, Lechleiter JD, Camacho P, 1998 Differential modulation of SERCA2 isoforms by calreticulin. *J Cell Biol* 142, 963–973. [PubMed: 9722609]
- Kamber D, Erez H, Spira ME, 2009 Local calcium-dependent mechanisms determine whether a cut axonal end assembles a retarded endbulb or competent growth cone. *Experimental neurology* 219, 112–125. 10.1016/j.expneurol.2009.05.004. [PubMed: 19442660]
- Kapur M, Monaghan CE, Ackerman SL, 2017 Regulation of mRNA Translation in Neurons-A Matter of Life and Death. *Neuron* 96, 616–637. 10.1016/j.neuron.2017.09.057. [PubMed: 29096076]
- Kaufman RJ, Davies MV, Pathak VK, Hershey JW, 1989 The phosphorylation state of eucaryotic initiation factor 2 alters translational efficiency of specific mRNAs. *Molecular and cellular biology* 9, 946–958. [PubMed: 2657393]
- Ketschek A, Gallo G, 2010 Nerve growth factor induces axonal filopodia through localized microdomains of phosphoinositide 3-kinase activity that drive the formation of cytoskeletal precursors to filopodia. *The Journal of neuroscience : the official journal of the Society for Neuroscience* 30, 12185–12197. 10.1523/JNEUROSCI.1740-10.2010.
- Kim KW, Jin Y, 2015 Neuronal responses to stress and injury in *C. elegans*. *FEBS letters* 589, 1644–1652. 10.1016/j.febslet.2015.05.005. [PubMed: 25979176]
- Kimball SR, 1999 Eukaryotic initiation factor eIF2. *The international journal of biochemistry & cell biology* 31, 25–29. [PubMed: 10216940]
- Kozak M, 1987 An analysis of 5'-noncoding sequences from 699 vertebrate messenger RNAs. *Nucleic acids research* 15, 8125–8148. [PubMed: 3313277]
- Kumar R, Azam S, Sullivan JM, Owen C, Cavener DR, Zhang P, Ron D, Harding HP, Chen JJ, Han A, White BC, Krause GS, DeGracia DJ, 2001 Brain ischemia and reperfusion activates the eukaryotic initiation factor 2 α kinase, PERK. *J Neurochem* 77, 1418–1421. [PubMed: 11389192]
- Lacerda R, Menezes J, Romao L, 2017 More than just scanning: the importance of cap-independent mRNA translation initiation for cellular stress response and cancer. *Cell Mol Life Sci* 74, 1659–1680. 10.1007/s00018-016-2428-2. [PubMed: 27913822]
- Li S, Yang L, Selzer ME, Hu Y, 2013 Neuronal endoplasmic reticulum stress in axon injury and neurodegeneration. *Ann Neurol* 74, 768–777. 10.1002/ana.24005. [PubMed: 23955583]
- Ma K, Vattem KM, Wek RC, 2002 Dimerization and release of molecular chaperone inhibition facilitate activation of eukaryotic initiation factor-2 kinase in response to endoplasmic reticulum stress. *The Journal of biological chemistry* 277, 18728–18735. 10.1074/jbc.M200903200. [PubMed: 11907036]
- MacLennan DH, Rice WJ, Green NM, 1997 The mechanism of Ca²⁺ transport by sarco(endo)plasmic reticulum Ca²⁺-ATPases. *The Journal of biological chemistry* 272, 28815–28818. [PubMed: 9360942]
- Merianda TT, Vuppalanchi D, Yoo S, Blesch A, Twiss JL, 2013 Axonal transport of neural membrane protein 35 mRNA increases axon growth. *J Cell Sci* 126, 90–102. 10.1242/jcs.107268. [PubMed: 23097042]
- Michalak M, Groenendyk J, Szabo E, Gold LI, Opas M, 2009 Calreticulin, a multi-process calcium-buffering chaperone of the endoplasmic reticulum. *Biochem J* 417, 651–666. 10.1042/BJ20081847. [PubMed: 19133842]
- Michalak M, Mariani P, Opas M, 1998 Calreticulin, a multifunctional Ca²⁺ binding chaperone of the endoplasmic reticulum. *Biochem Cell Biol* 76, 779–785. [PubMed: 10353711]
- Michalak M, Robert Parker JM, Opas M, 2002 Ca²⁺ signaling and calcium binding chaperones of the endoplasmic reticulum. *Cell Calcium* 32, 269–278. [PubMed: 12543089]
- Molinari M, Eriksson KK, Calanca V, Galli C, Cresswell P, Michalak M, Helenius A, 2004 Contrasting functions of calreticulin and calnexin in glycoprotein folding and ER quality control. *Mol Cell* 13, 125–135. [PubMed: 14731400]

- Moolenaar WH, van Meeteren LA, Giepmans BN, 2004 The ins and outs of lysophosphatidic acid signaling. *Bioessays* 26, 870–881. 10.1002/bies.20081. [PubMed: 15273989]
- Moon SL, Sonenberg N, Parker R, 2018 Neuronal Regulation of eIF2alpha Function in Health and Neurological Disorders. *Trends Mol Med* 24, 575–589. 10.1016/j.molmed.2018.04.001. [PubMed: 29716790]
- Moore MJ, 2005 From birth to death: the complex lives of eukaryotic mRNAs. *Science* 309, 1514–1518. 10.1126/science.1111443. [PubMed: 16141059]
- Fukushima N, 2011 Microtubules in the nervous system, in: Nixon RA, Yuan A (Ed.), *Cytoskeleton in the Nervous System*. Springer, New York, pp. 55–71.
- Ohtake Y, Matsuhisa K, Kaneko M, Kanemoto S, Asada R, Imaizumi K, Saito A, 2018 Axonal Activation of the Unfolded Protein Response Promotes Axonal Regeneration Following Peripheral Nerve Injury. *Neuroscience* 375, 34–48. 10.1016/j.neuroscience.2018.02.003. [PubMed: 29438804]
- Onate M, Catenaccio A, Martinez G, Armentano D, Parsons G, Kerr B, Hetz C, Court FA, 2016 Activation of the unfolded protein response promotes axonal regeneration after peripheral nerve injury. *Sci Rep* 6, 21709 10.1038/srep21709. [PubMed: 26906090]
- Ostwald TJ, MacLennan DH, 1974 Isolation of a high affinity calcium-binding protein from sarcoplasmic reticulum. *The Journal of biological chemistry* 249, 974–979. [PubMed: 4272851]
- Owen CR, Kumar R, Zhang P, McGrath BC, Cavener DR, Krause GS, 2005 PERK is responsible for the increased phosphorylation of eIF2alpha and the severe inhibition of protein synthesis after transient global brain ischemia. *J Neurochem* 94, 1235–1242. 10.1111/j.1471-4159.2005.03276.x. [PubMed: 16000157]
- Lelkes P.I., Unsworth BR, Saporta S, Cameron DF, Gallo G, 2006 Culture of neuroendocrine and neuronal cells for tissue engineering, in: Vunjak-Novakovic G, Freshney RI (Eds.), *Culture of cells for tissue engineering*. Wiley-Liss, New Jersey, pp. 375–415.
- Pacheco A, Twiss JL, 2012 Localized IRES-dependent translation of ER chaperone protein mRNA in sensory axons. *PloS one* 7, e40788 10.1371/journal.pone.0040788. [PubMed: 22911708]
- Pakos-Zebrucka K, Koryga I, Mnich K, Ljubic M, Samali A, Gorman AM, 2016 The integrated stress response. *EMBO Rep* 17, 1374–1395. 10.15252/embr.201642195. [PubMed: 27629041]
- Pathak VK, Schindler D, Hershey JW, 1988 Generation of a mutant form of protein synthesis initiation factor eIF-2 lacking the site of phosphorylation by eIF-2 kinases. *Molecular and cellular biology* 8, 993–995. [PubMed: 3352609]
- Perlson E, Hanz S, Ben-Yaakov K, Segal-Ruder Y, Seger R, Fainzilber M, 2005 Vimentin-dependent spatial translocation of an activated MAP kinase in injured nerve. *Neuron* 45, 715–726. 10.1016/j.neuron.2005.01.023. [PubMed: 15748847]
- Perry RB, Fainzilber M, 2009 Nuclear transport factors in neuronal function. *Semin Cell Dev Biol* 20, 600–606. 10.1016/j.semcdb.2009.04.014. [PubMed: 19409503]
- Pinan-Lucarre B, Gabel CV, Reina CP, Hulme SE, Shevkoplyas SS, Slone RD, Xue J, Qiao Y, Weisberg S, Roodhouse K, Sun L, Whitesides GM, Samuel A, Driscoll M, 2012 The core apoptotic executioner proteins CED-3 and CED-4 promote initiation of neuronal regeneration in *Caenorhabditis elegans*. *PLoS Biol* 10, e1001331 10.1371/journal.pbio.1001331. [PubMed: 22629231]
- Platika D, Boulos MH, Baizer L, Fishman MC, 1985 Neuronal traits of clonal cell lines derived by fusion of dorsal root ganglia neurons with neuroblastoma cells. *Proc Natl Acad Sci U S A* 82, 3499–3503. [PubMed: 3858835]
- Raven JF, Koromilas AE, 2008 PERK and PKR: old kinases learn new tricks. *Cell Cycle* 7, 1146–1150. 10.4161/cc.7.9.5811. [PubMed: 18418049]
- Reid DW, Chen Q, Tay AS, Shenolikar S, Nicchitta CV, 2014 The unfolded protein response triggers selective mRNA release from the endoplasmic reticulum. *Cell* 158, 1362–1374. 10.1016/j.cell.2014.08.012. [PubMed: 25215492]
- Rigaud M, Gemes G, Weyker PD, Cruikshank JM, Kawano T, Wu HE, Hogan QH, 2009 Axotomy depletes intracellular calcium stores in primary sensory neurons. *Anesthesiology* 111, 381–392. 10.1097/ALN.0b013e3181ae6212. [PubMed: 19602958]

- Sekine Y, Zyryanova A, Crespillo-Casado A, Fischer PM, Harding HP, Ron D, 2015 Stress responses. Mutations in a translation initiation factor identify the target of a memory-enhancing compound. *Science* 348, 1027–1030. 10.1126/science.aaa6986. [PubMed: 25858979]
- Shi Y, Vattem KM, Sood R, An J, Liang J, Stramm L, Wek RC, 1998 Identification and characterization of pancreatic eukaryotic initiation factor 2 alpha-subunit kinase, PEK, involved in translational control. *Molecular and cellular biology* 18, 7499–7509. 10.1128/mcb.18.12.7499. [PubMed: 9819435]
- Shih YY, Nakagawara A, Lee H, Juan HF, Jeng YM, Lin DT, Yang YL, Tsay YG, Huang MC, Pan CY, Hsu WM, Liao YF, 2012 Calreticulin mediates nerve growth factor-induced neuronal differentiation. *J Mol Neurosci* 47, 571–581. 10.1007/s12031-011-9683-3. [PubMed: 22147490]
- Smith DS, Skene JH, 1997 A transcription-dependent switch controls competence of adult neurons for distinct modes of axon growth. *The Journal of neuroscience : the official journal of the Society for Neuroscience* 17, 646–658. [PubMed: 8987787]
- Spillane M, Ketschek A, Donnelly CJ, Pacheco A, Twiss JL, Gallo G, 2012 Nerve growth factor-induced formation of axonal filopodia and collateral branches involves the intra-axonal synthesis of regulators of the actin-nucleating Arp2/3 complex. *The Journal of neuroscience : the official journal of the Society for Neuroscience* 32, 17671–17689. 10.1523/JNEUROSCI.1079-12.2012. [PubMed: 23223289]
- Spriggs KA, Bushell M, Willis AE, 2010 Translational regulation of gene expression during conditions of cell stress. *Mol Cell* 40, 228–237. 10.1016/j.molcel.2010.09.028. [PubMed: 20965418]
- Spriggs KA, Stoneley M, Bushell M, Willis AE, 2008 Re-programming of translation following cell stress allows IRES-mediated translation to predominate. *Biol Cell* 100, 27–38. 10.1042/BC20070098. [PubMed: 18072942]
- Su Q, Wang S, Gao HQ, Kazemi S, Harding HP, Ron D, Koromilas AE, 2008 Modulation of the eukaryotic initiation factor 2 alpha-subunit kinase PERK by tyrosine phosphorylation. *The Journal of biological chemistry* 283, 469–475. 10.1074/jbc.M704612200. [PubMed: 17998206]
- Tushev G, Glock C, Heumuller M, Biever A, Jovanovic M, Schuman EM, 2018 Alternative 3' UTRs Modify the Localization, Regulatory Potential, Stability, and Plasticity of mRNAs in Neuronal Compartments. *Neuron* 98, 495–511 e496. 10.1016/j.neuron.2018.03.030. [PubMed: 29656876]
- Twiss JL, Smith DS, Chang B, Shooter EM, 2000 Translational control of ribosomal protein L4 mRNA is required for rapid neurite regeneration. *Neurobiol Dis* 7, 416–428. 10.1006/nbdi.2000.0293. [PubMed: 10964612]
- Verma P, Chierzi S, Codd AM, Campbell DS, Meyer RL, Holt CE, Fawcett JW, 2005 Axonal protein synthesis and degradation are necessary for efficient growth cone regeneration. *The Journal of neuroscience : the official journal of the Society for Neuroscience* 25, 331–342. 10.1523/JNEUROSCI.3073-04.2005. [PubMed: 15647476]
- Vogelaar CF, Gervasi NM, Gumy LF, Story DJ, Raha-Chowdhury R, Leung KM, Holt CE, Fawcett JW, 2009 Axonal mRNAs: characterisation and role in the growth and regeneration of dorsal root ganglion axons and growth cones. *Molecular and cellular neurosciences* 42, 102–115. 10.1016/j.mcn.2009.06.002. [PubMed: 19520167]
- Vuppalanchi D, Coleman J, Yoo S, Merianda TT, Yadhati AG, Hossain J, Blesch A, Willis DE, Twiss JL, 2010 Conserved 3'-untranslated region sequences direct subcellular localization of chaperone protein mRNAs in neurons. *The Journal of biological chemistry* 285, 18025–18038. 10.1074/jbc.M109.061333. [PubMed: 20308067]
- Vuppalanchi D, Merianda TT, Donnelly C, Pacheco A, Williams G, Yoo S, Ratan RR, Willis DE, Twiss JL, 2012 Lysophosphatidic acid differentially regulates axonal mRNA translation through 5'UTR elements. *Molecular and cellular neurosciences* 50, 136–146. 10.1016/j.mcn.2012.04.001. [PubMed: 22522146]
- Vuppalanchi D, Willis DE, Twiss JL, 2009 Regulation of mRNA transport and translation in axons. *Results Probl Cell Differ* 48, 193–224. 10.1007/400_2009_16. [PubMed: 19582411]
- Wang JT, Medress ZA, Barres BA, 2012 Axon degeneration: molecular mechanisms of a self-destruction pathway. *J Cell Biol* 196, 7–18. 10.1083/jcb.201108111. [PubMed: 22232700]

- Wang W, van Niekerk E, Willis DE, Twiss JL, 2007 RNA transport and localized protein synthesis in neurological disorders and neural repair. *Dev Neurobiol* 67, 1166–1182. 10.1002/dneu.20511. [PubMed: 17514714]
- Willis D, Li KW, Zheng JQ, Chang JH, Smit AB, Kelly T, Merianda TT, Sylvester J, van Minnen J, Twiss JL, 2005 Differential transport and local translation of cytoskeletal, injury-response, and neurodegeneration protein mRNAs in axons. *The Journal of neuroscience : the official journal of the Society for Neuroscience* 25, 778–791. 10.1523/JNEUROSCI.4235-04.2005. [PubMed: 15673657]
- Willis DE, van Niekerk EA, Sasaki Y, Mesngon M, Merianda TT, Williams GG, Kendall M, Smith DS, Bassell GJ, Twiss JL, 2007 Extracellular stimuli specifically regulate localized levels of individual neuronal mRNAs. *J Cell Biol* 178, 965–980. 10.1083/jcb.200703209. [PubMed: 17785519]
- Ye X, Fukushima N, Kingsbury MA, Chun J, 2002 Lysophosphatidic acid in neural signaling. *Neuroreport* 13, 2169–2175. [PubMed: 12488791]
- Yudin D, Hanz S, Yoo S, Iavnilovitch E, Willis D, Gradus T, Vuppalanchi D, Segal-Ruder Y, Ben-Yaakov K, Hieda M, Yoneda Y, Twiss JL, Fainzilber M, 2008 Localized regulation of axonal RanGTPase controls retrograde injury signaling in peripheral nerve. *Neuron* 59, 241–252. 10.1016/j.neuron.2008.05.029. [PubMed: 18667152]
- Zheng JQ, Kelly TK, Chang B, Ryazantsev S, Rajasekaran AK, Martin KC, Twiss JL, 2001 A functional role for intra-axonal protein synthesis during axonal regeneration from adult sensory neurons. *The Journal of neuroscience : the official journal of the Society for Neuroscience* 21, 9291–9303. [PubMed: 11717363]

Highlights

- Axotomy increase axonal Calreticulin translation in the PNS
- Injury induced PERK-dependent Phospho-eIF2 α triggers axonal Calreticulin translation
- Control of Calreticulin translation in axons requires both 5' and 3'UTR mRNA motifs
- Calreticulin translation in cut axons reduces retraction and facilitates regeneration

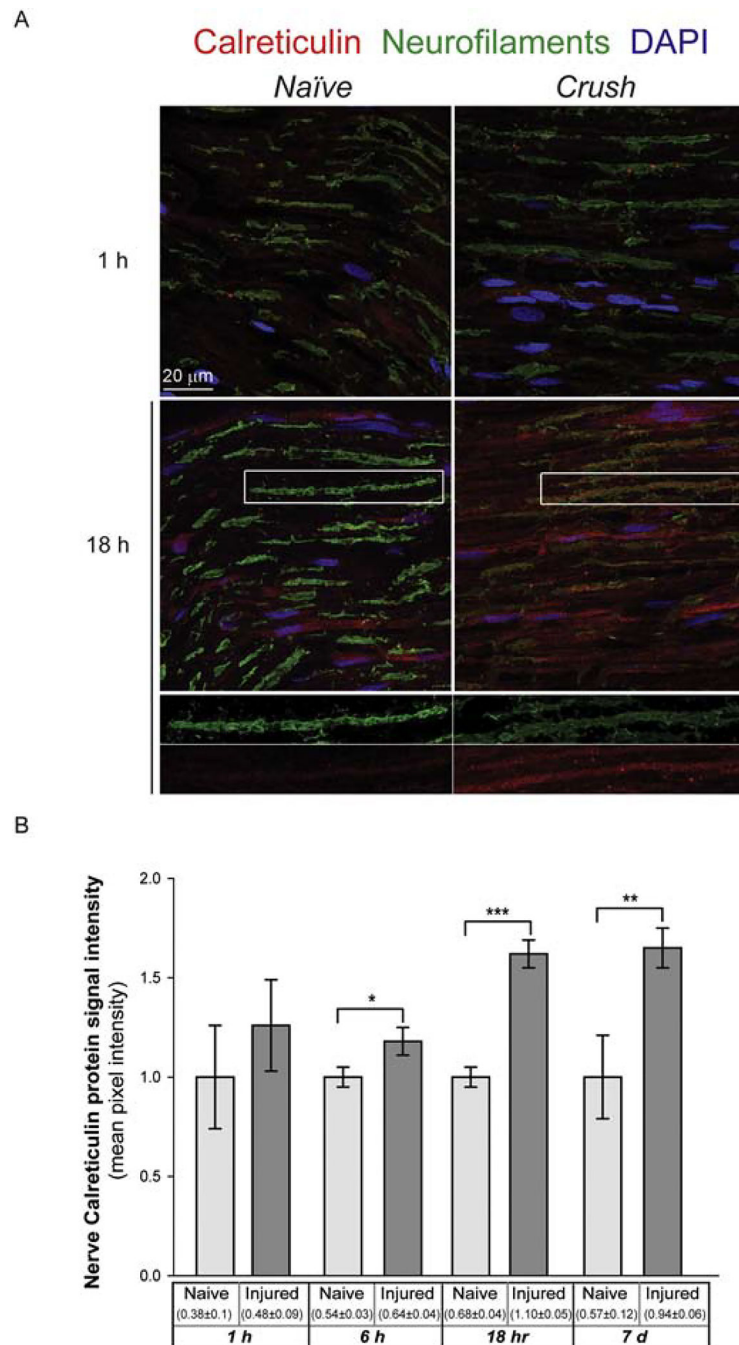


Figure 1. Axonal injury increases the axonal levels of Calreticulin protein in vivo.

A, Representative exposure-matched confocal images of IF signals for naïve (control) vs. 1 h and 18 h post-crush-injury sciatic nerve are shown. Calreticulin protein is displayed in red color, NF protein is displayed in green color and DAPI in blue color. The merged channels are shown in the main panels of naïve and 1 h and 18 h post-crush-injury sciatic nerve and the white rectangles indicate magnification views of the Calreticulin and NF signals that are shown in the lower panels of 18 h post-crush-injury sciatic nerve. Intra-axonal Calreticulin protein signal is seen in both the naïve (control) and injured nerve sections. **B**,

Quantification of Calreticulin protein (red signal) mean pixel intensity overlapping with NF H signal (green) in uninjured and injured sciatic nerve at 1 h, 6 h, 18 h and 7 days after injury is shown as the fold change relative to naïve as Mean \pm SEM (*P 0.05; **P 0.01; ***P 0.001 by Student's T-test). The levels of Calreticulin within time points are presented normalized to the time matched control group. The signal of axonal Calreticulin protein starts to increase at 6 h after injury over 7 days post-crush-injury sciatic nerve in compare with the control, reaching the maximum statistical significance at 18 h post-injury.

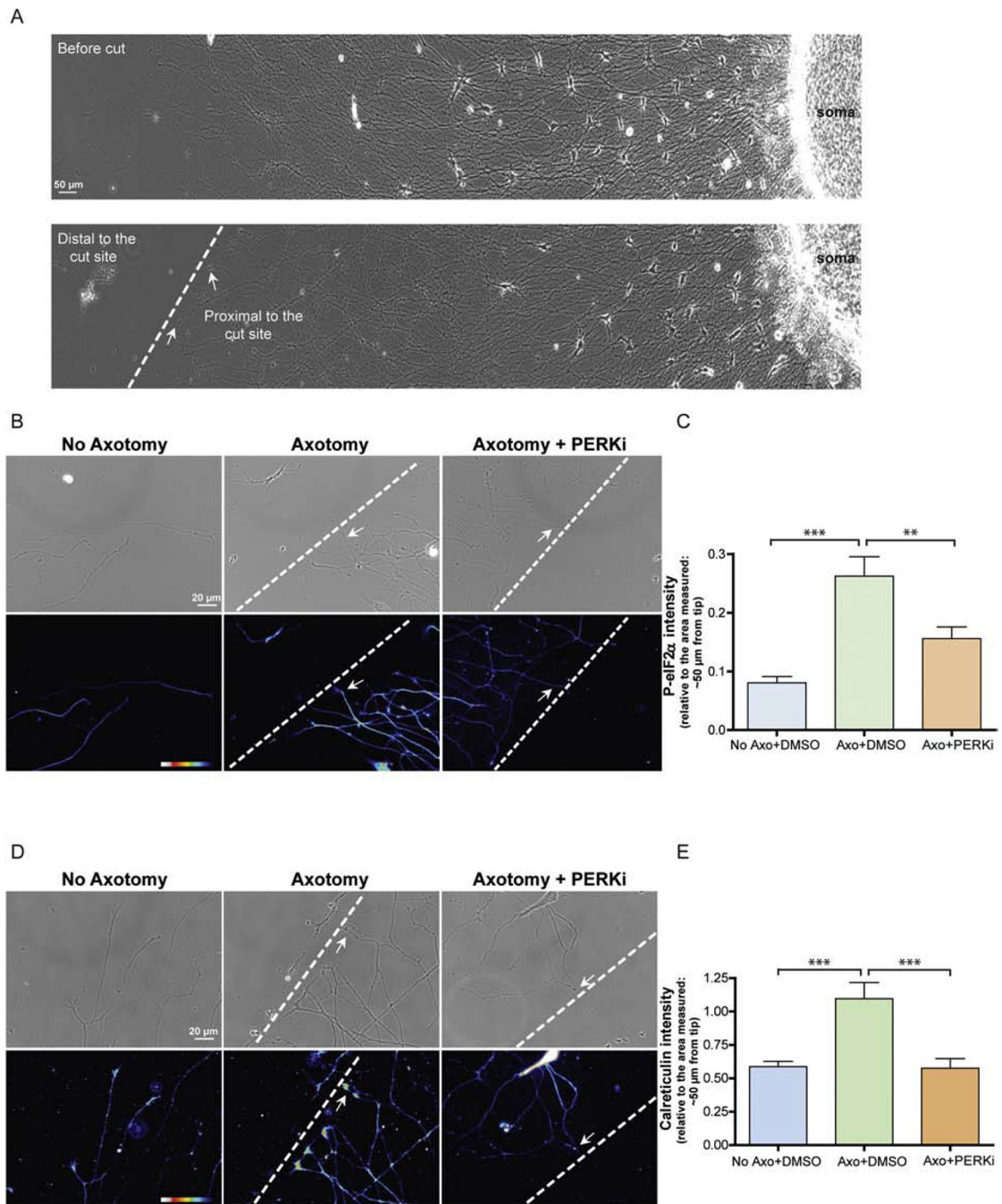


Figure 2. Axonal injury increases eIF2 α phosphorylation and Calreticulin levels.

A, Distal axons of chicken DRG explants were cut 24 h after culture at 800 – 1000 μ m from the soma. The dotted line represents the site of axotomy, the arrows indicate examples of the growing axons. The samples were pretreated 10–15 min before axotomy with PERK inhibitor (GSK2606414, 90 μ M) or the vehicle DMSO and they were processed 20 min after axotomy for immunostaining with antibodies to P-eIF2 α (Ser51) (**B**) or to Calreticulin (**D**). **B**, Exposure matched images of distal axons are shown for the immunoreactivity to P-eIF2 α (Ser51). The arrows indicate examples of the growing axons after 20 min of axotomy and

the dotted line represent the area of axotomy. **C**, Quantification of the integrated background subtracted staining intensities of eIF2 α -pS51 in the cut end of the axons (ROI 30–50 μ m from severed tip toward the distal axon attached to the soma) are shown in the graph as an average of fluorescence intensity \pm SEM (n = 42 axons (*No Axotomy*), n = 42 axons (*Axotomy*) and n = 46 axons (*Axotomy + PERKi*); *** p 0.001, ** p 0.01 by Mann-Whitney test). The levels of phosphorylated eIF2 α were significantly increased. Pre-treatment of the DRG explants with PERK inhibitor significantly decreased the levels of P-eIF2 α in response to axotomy. **D**, Exposure matched images of distal axons are shown for the immunoreactivity to Calreticulin. **E**, Quantification of the integrated staining intensity of Calreticulin in the cut end of the distal axons (ROI 30–50 μ m from severed tip) are shown in the graph as an average of fluorescence intensity \pm SEM (n = 51 axons (*No Axotomy*), n = 44 axons (*Axotomy*) and n = 51 axons (*Axotomy + PERKi*). Comparison of the indicated groups yield *** p 0.001 by Mann-Whitney test. The levels of Calreticulin were significantly increased after 20 min of axotomy. Pre-treatment of the DRG explants with PERK inhibitor significantly decreased the levels of Calreticulin in response to axotomy.

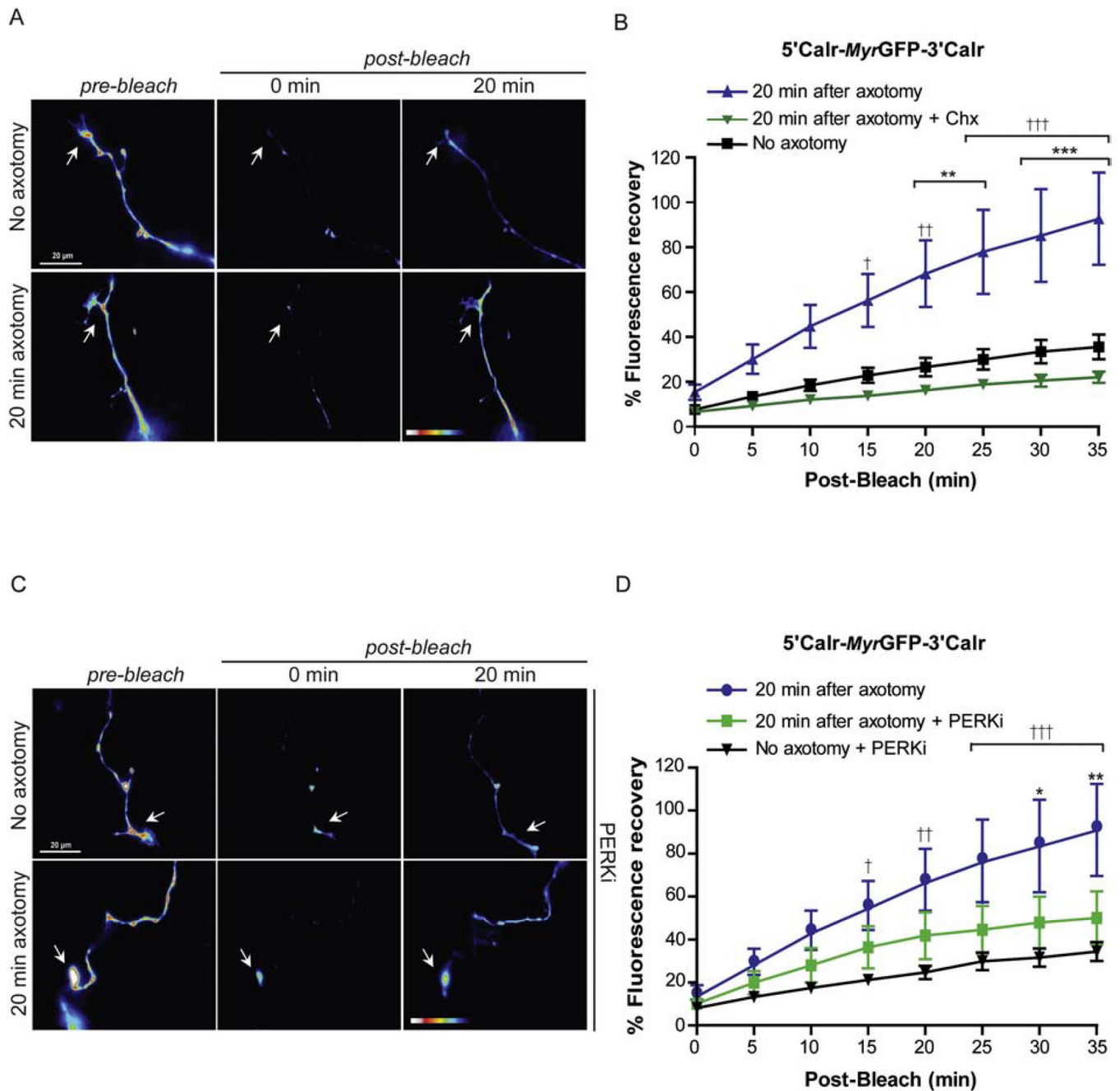


Figure 3. Injury triggers axonal Calreticulin translation in response to injury through PERK signaling.

A, Representative false colored axons showing time-lapse sequences from FRAP analyses of DRG axons are shown 20 min after axotomy before bleaching (pre-bleach) and after bleaching (post-bleach). **B**, The signals in the series are measured in a 30–50 μm ROI from the axon tip (white arrow) toward the distal shaft of the cut axon remaining attached to the soma. The quantified signals are normalized to pre-bleach levels and expressed as average percent prebleach signals \pm SEM ($n = 10$ over at least 4 independent transfections). Comparison of fluorescence signals of axotomized DRG neurons expressing 5'Calr-

MyrGFP-3'Calr versus fluorescence signals of not axotomized neurons expressing 5'Calr-*MyrGFP-3'Calr* yielded **p 0.01, and ***p 0.001 for time points shown in the graph. Comparison of fluorescence signals of axotomized DRG neurons expressing 5'Calr-*MyrGFP-3'Calr* versus axotomized neurons pretreated with cycloheximide and expressing 5'Calr-*MyrGFP-3'Calr* yielded † p 0.05, †† p 0.01, and ††† p 0.001 for time points shown in the graph. By two-way ANOVA compared to t = 0 min post-bleach. The translation of 5'Calr-*MyrGFP-3'Calr* mRNA was upregulated at the end of the cut axons, remaining attached to the soma in comparison with the non-injured distal axons. **C**, Representative false colored axons showing time-lapse sequences from FRAP analyses of DRG neurons are shown 20 min after axotomy before bleaching (pre-bleach) and after bleaching (post-bleach) (see panels on A as an example of fluorescence recovery 20 min after axotomy with no drug treatment). Pre-treatment with PERK inhibitor (GSK2606414, 800 nM) is indicated in the corresponding panels. **D**, The signals in the series are measured in a 30–50 μm ROI from the axon tip toward the distal shaft of the cut axon remaining attached to the soma. The quantified signals are normalized to pre-bleach levels and are expressed as average percent prebleach signals ± SEM (n = 10 over at least 4 independent transfections). Comparison of fluorescence signals of axotomized DRG neurons expressing 5'Calr-*MyrGFP-3'Calr* versus axotomized neurons pre-treated with PERK inhibitor and expressing 5'Calr-*MyrGFP-3'Calr* yielded *p 0.05, **p 0.01 for time points shown in the graph. Comparison of fluorescence signals of axotomized DRG neurons expressing 5'Calr-*MyrGFP-3'Calr* versus not axotomized neurons pre-treated with PERK inhibitor and expressing 5'Calr-*MyrGFP-3'Calr* yielded † p 0.05, †† p 0.01, and ††† p 0.001 for time points shown in the graph. By two-way ANOVA compared to t = 0 min post-bleach. The axonal recovery of the signal was significantly decreased in axotomized-neurons pre-treated with GSK2606414 and the basal translation of 5'Calr-*MyrGFP-3'Calr* mRNA in not axotomized neurons was not affected for the treatment with PERK inhibitor (ns, P > 0.05) (compare Fig. 3B no axotomy and Fig. 3D no axotomy + PERKi).

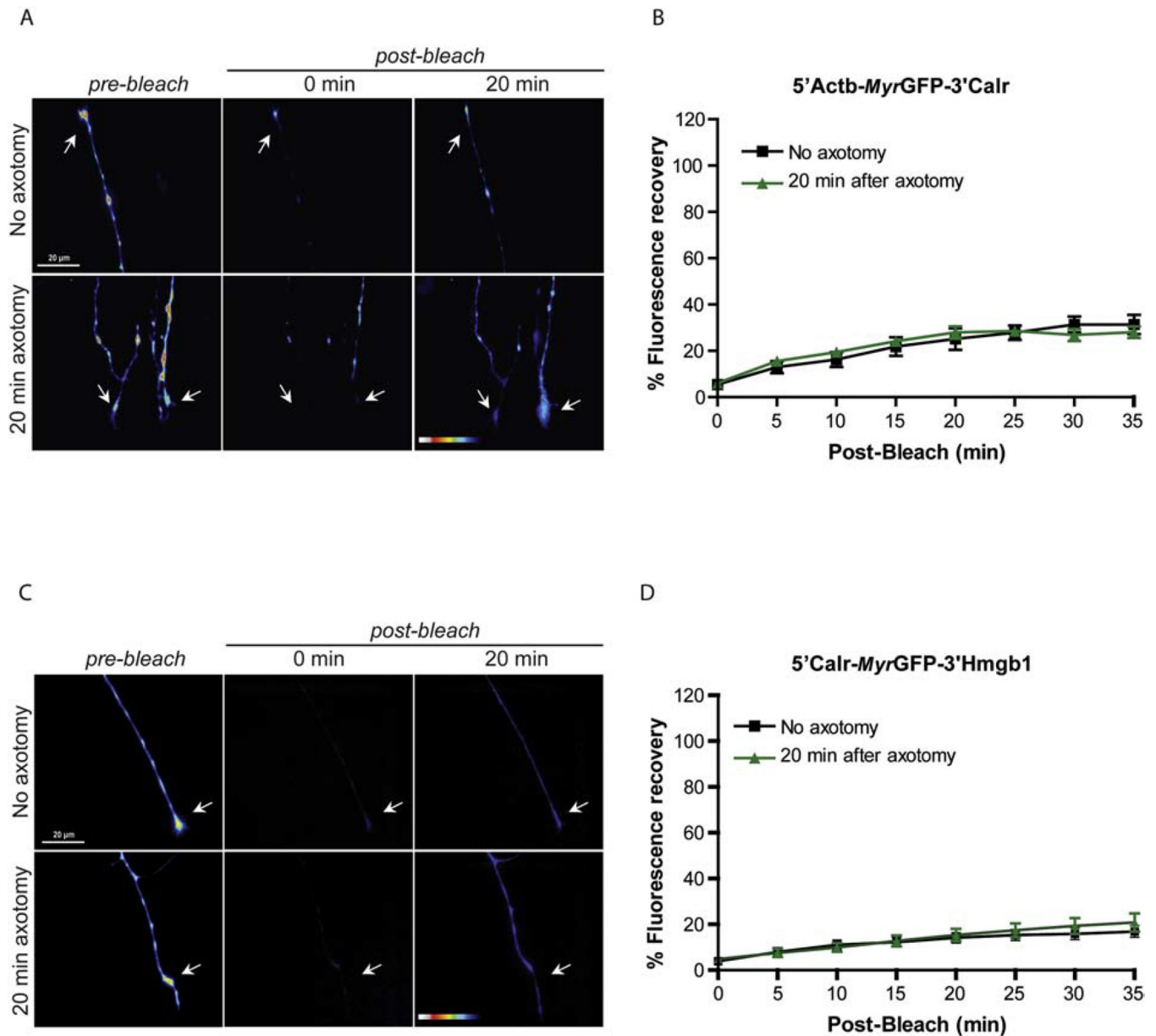


Figure 4. Both Calreticulin 5'UTR and 3'UTR mRNA elements are required for axonal translation in response to injury.

A, Representative false colored axons from time-lapse sequences of FRAP analyses of DRG neurons transfected with the indicated plasmid are shown 20 min after axotomy before and after bleaching. **B**, The signals in the series are measured in a 30–50 μm ROI from the axon tip toward the distal shaft of the cut axon remaining attached to the soma. The quantified signals are normalized to pre-bleach levels and are expressed as average percent prebleach signals \pm SEM ($n = 9$ over at least 4 independent transfections). Comparison of fluorescence signals of axotomized DRG neurons expressing 5'Actb-MyrGFP-3'Calr versus not axotomized DRG neurons expressing 5'Actb-MyrGFP-3'Calr was overall no significant ($P > 0.05$). By two-way ANOVA compared to $t = 0$ min post-bleach. Cut axons of DRG neurons expressing and mRNA lacking of Calr 5'UTR were not able to trigger Calreticulin

axonal translation in response to injury. **C**, Representative false colored axons from time-lapse sequences of FRAP analyses of DRG neurons transfected with the indicated plasmid are shown 20 min after axotomy before and after bleaching. **D**, The signals in the series are measured in a 30–50 μm ROI from the axon tip toward the distal shaft of the cut axon remaining attached to the soma. The quantified signals are normalized to pre-bleach levels and are expressed as average percent prebleach signals \pm SEM ($n = 12$ over at least 4 independent transfections). Comparison of fluorescence signals of axotomized DRG neurons expressing 5'Calr-MyrGFP-3'Hmgb1 versus not axotomized DRG neurons expressing 5'Calr-MyrGFP-3'Hmgb1 was overall no significant ($P > 0.05$). By two-way ANOVA compared to $t = 0$ min post-bleach. Cut axons of DRG neurons expressing and mRNA lacking of Calr 3'UTR were not able to trigger Calreticulin axonal translation in response to injury.

Author Manuscript

Author Manuscript

Author Manuscript

Author Manuscript

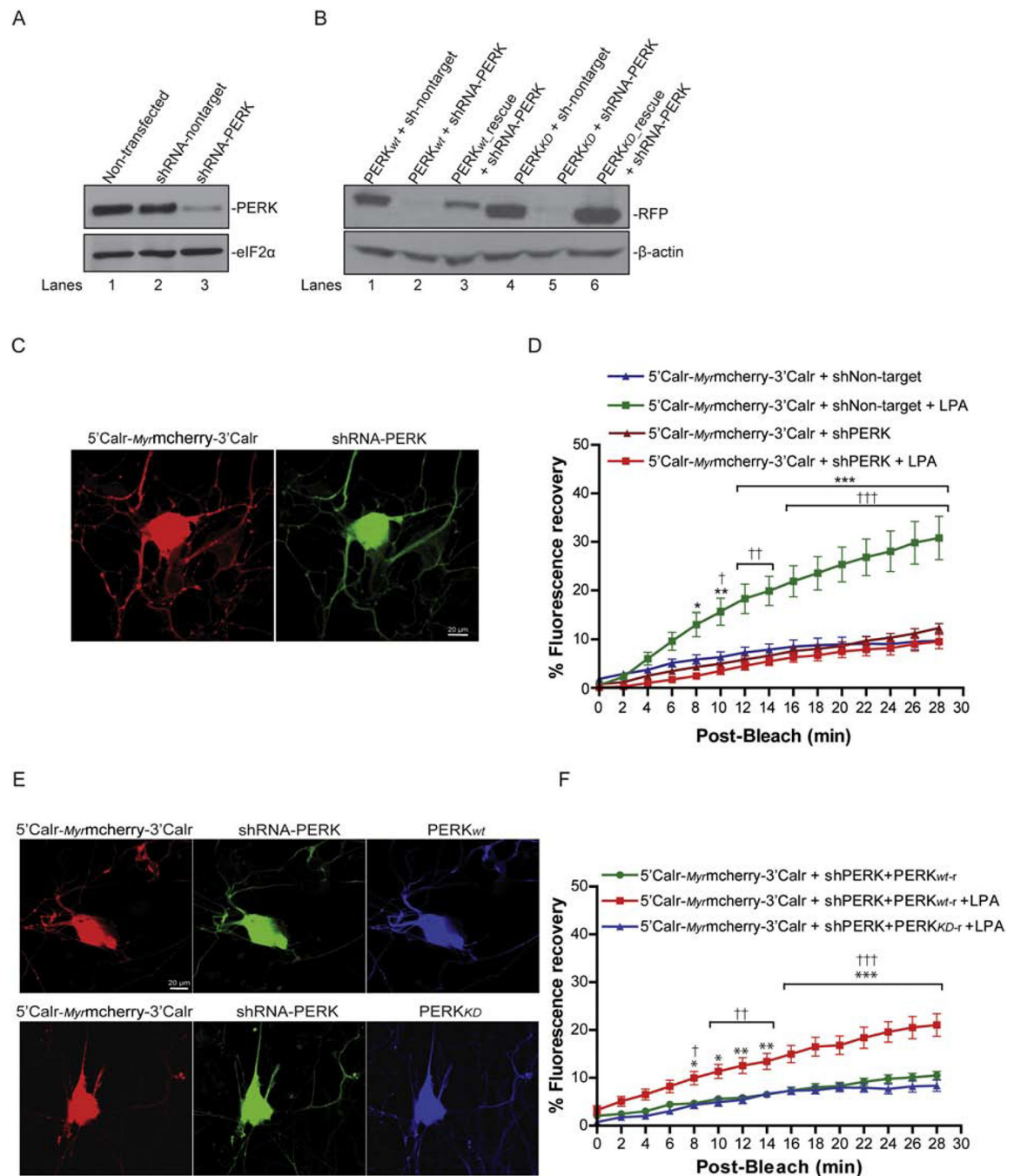


Figure 5. PERK is required for the synthesis of axonal Calreticulin in response to ER stress.

A, A western blot panel shows in the first row the decreased endogenous level of PERK 48 h after transfection of F11 cells with the plasmid pSUPERshRNA-PERK-GFP. As a loading control, total eIF2 α signal is shown in the second row. **B**, A western blot panel shows in the first row the decreased endogenous level of exogenous recombinant proteins PERK_{wt}-BFP/ pPERK_{wt}.rescue-BFP or pPERK_{kd}-BFP/ pPERK_{kd}.rescue-BFP after co-transfection of F11 cells with the plasmids pSUPERshRNA-PERK-GFP or pSUPERshRNA-nontarget-GFP. As a loading control, β -actin signal is shown in the second row. **C**, Representative static

images of DRG neurons co-expressing 5'Calr-*Mymcherry*-3'Calr (red signal) and shRNA-PERK (green signal) are shown 48 h post-transfection. Both mCherry (red, left panel) and GFP (green, right panel) signals are observed in the cell bodies and in the axons of the neurons. **D**, The signals in the series are measured in a 30–50 μm ROI from the axon tip toward the distal shaft of the cut axon remaining attached to the soma. The quantified signals are normalized to pre-bleach levels and are expressed as average percent prebleach signals \pm SEM (n = 10 over at least 4 independent transfections). Comparison of fluorescence signals of neurons expressing 5'Calr-*Mymcherry*-3'Calr and the shRNA-nontarget versus LPA pre-treated DRG neurons expressing 5'Calr-*Mymcherry*-3'Calr and the shRNA-nontarget yielded \dagger p = 0.05, $\dagger\dagger$ p = 0.01, and $\dagger\dagger\dagger$ p = 0.001 for time points shown in the graph. Comparison of fluorescence signals of LPA pre-treated DRG neurons expressing 5'Calr-*Mymcherry*-3'Calr and the shRNA-nontarget versus LPA pre-treated DRG neurons expressing 5'Calr-*Mymcherry*-3'Calr and the shRNA-PERK yielded *p = 0.05, **p = 0.01 and ***p = 0.001 for time points shown in the graph. Comparison of fluorescence signals of neurons expressing 5'Calr-*Mymcherry*-3'Calr and the shRNA-nontarget versus neurons expressing 5'Calr-*Mymcherry*-3'Calr and the shRNA-PERK or versus LPA pre-treated DRG neurons expressing 5'Calr-*Mymcherry*-3'Calr and the shRNA-PERK were overall no significant ($P > 0.05$). By two-way ANOVA compared to t = 0 min post-bleach. PERK knockdown were not able to trigger axonal translation in response to LPA treatment. **E**, Representative static images of DRG neurons co-expressing 5'Calr-*Mymcherry*-3'Calr, shRNA-PERK and PERK_{wt} or PERK_{KD} proteins are shown at 48 h post-transfection in the first and the second row respectively. mCherry (red signal, left panels), GFP (green signal, middle panels) and BFP (blue signal, right panels) fluorescence is seen in the cell bodies and in the axons of the neurons. **F**, The signals in the series are measured in a 30–50 μm ROI from the axon tip toward the distal shaft of the cut axon remaining attached to the soma. The quantified signals are normalized to pre-bleach levels and are expressed as average percent prebleach signals \pm SEM (n = 11 over at least 4 independent transfections). Comparison of neurons co-expressing 5'Calr-*Mymcherry*-3'Calr, the shRNA-PERK and the PERK_{wt-r} versus LPA treated DRG neurons coexpressing 5'Calr-*Mymcherry*-3'Calr, the shRNA-PERK and the PERK_{wt-r} yielded *p = 0.05, **p = 0.01 and ***p = 0.001 for time points shown in the graph. Comparison of LPA treated DRG neurons co-expressing 5'Calr-*Mymcherry*-3'Calr, the shRNA-PERK and the PERK_{wt-r} versus LPA treated neurons co-expressing 5'Calr-*Mymcherry*-3'Calr, the shRNA-PERK and the PERK_{KD-r} yielded \dagger p = 0.05, $\dagger\dagger$ p = 0.01, and $\dagger\dagger\dagger$ p = 0.001 for time points shown in the graph. Comparison of neurons co-expressing 5'Calr-*Mymcherry*-3'Calr, the shRNA-PERK and the PERK_{wt-r} versus LPA treated DRG neurons coexpressing 5'Calr-*Mymcherry*-3'Calr, the shRNA-PERK and the PERK_{KD-r} was overall no significant ($P > 0.05$). By two-way ANOVA compared to t = 0 min post-bleach. Only those neurons expressing an active PERK were able to respond to LPA-mediated translation in PERK knockdown neurons.

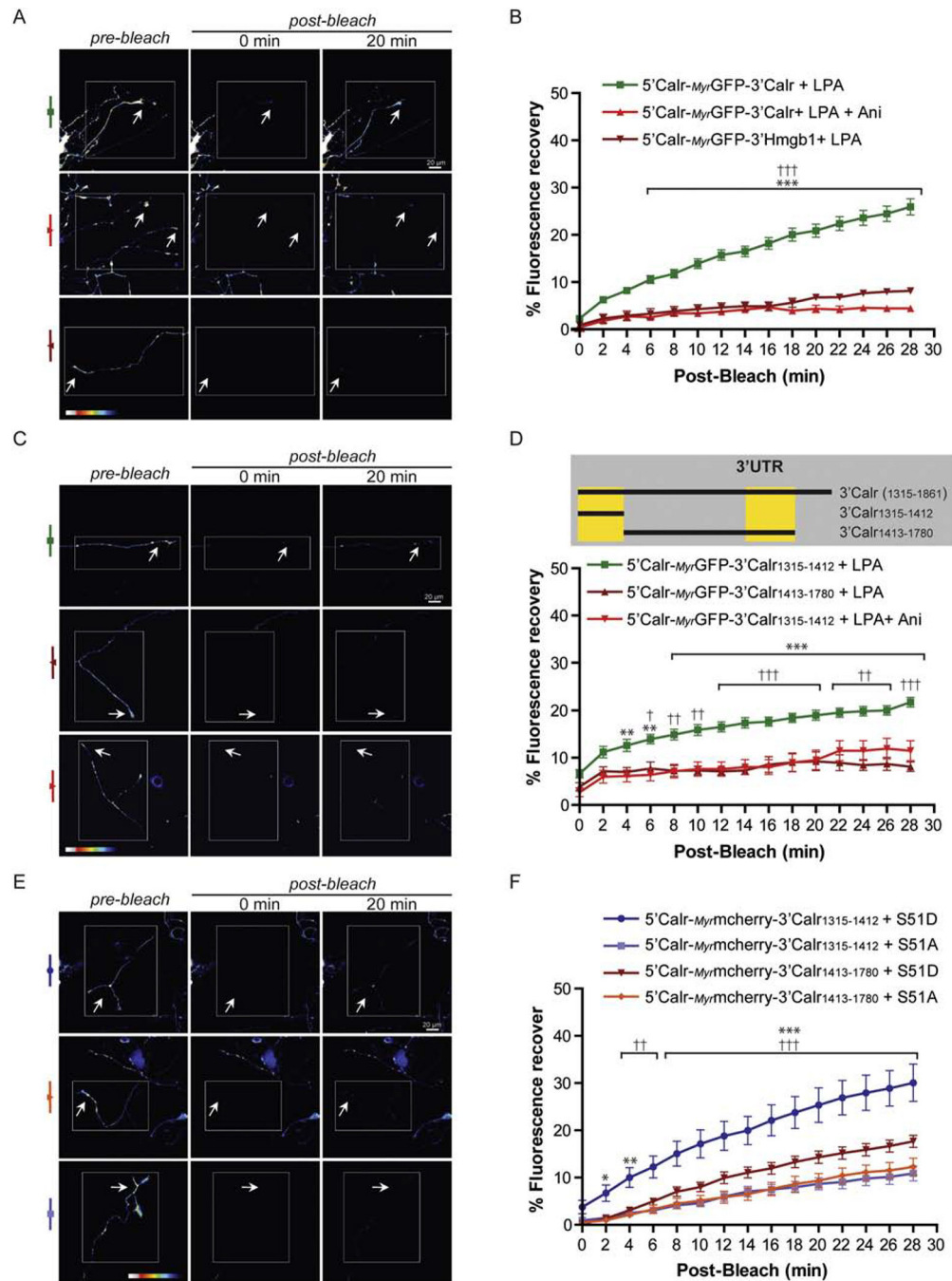


Figure 6. 5'UTR and 3'UTR elements are necessary for axonal translation of Calreticulin mRNA in response to eIF2 α phosphorylation.

A, Representative false colored axons showing time-lapse sequences from FRAP analyses of DRG neurons transfected with the indicated plasmids are shown before and after bleaching. The white boxed regions represent the regions subjected to photobleaching and the arrows indicate the regions of the terminal axon where the recovery signal was quantified. **B**, The signals in the series are measured in a 30–50 μm ROI from the axon tip toward the distal shaft of the cut axon remaining attached to the soma. The quantified signals are normalized

to pre-bleach levels and are expressed as average percent prebleach signals \pm SEM (n = 12 over at least 4 independent transfections). Comparison of DRG neurons treated with LPA and expressing 5'Calr-MyrGFP-3'Calr versus neurons treated with LPA + anisomycin and expressing 5'Calr-MyrGFP-3'Calr yielded ***p = 0.001 for time points shown in the graph. Comparison of DRG neurons treated with LPA and expressing 5'Calr-MyrGFP-3'Calr versus neurons treated with LPA and expressing 5'Calr-MyrGFP-3' Hmgb1 yielded ††† p = 0.001 for time points shown in the graph. By two-way ANOVA compared to t = 0 min post-bleach. **C**, Representative false colored axons showing time-lapse sequences from FRAP analyses of DRG neurons transfected with the indicated plasmids are shown before and after bleaching. The white boxed regions represent the regions subjected to photobleaching and the arrows indicate the regions of the terminal axon where recovery was quantified. **D**, The diagram above the graph shows schematically the regions of the rat Calreticulin 3'UTR that were tested for axonal Calreticulin translation in the FRAP analysis. Based on previous data (Vuppalanchi et al., 2010), either of the two regions highlighted in yellow suffice as the minimum sequence sufficient to target the indicated mRNAs into axons of cultured DRG neuron. The signals in the series are measured in a 30–50 μ m ROI from the axon tip toward the distal shaft of the cut axon remaining attached to the soma. The quantified signals are normalized to pre-bleach levels and are expressed as average percent prebleach signals \pm SEM (n = 8 over at least 4 independent transfections). Comparison of DRG neurons treated with LPA and expressing 5'Calr-MyrGFP-3'Calr_{1315–1412} versus neurons treated with LPA and expressing 5'Calr-MyrGFP-3'Calr_{1413–1780} yielded **p = 0.01, and ***p = 0.001 for time points shown in the graph. Comparison of DRG neurons treated with LPA and expressing 5'Calr-MyrGFP-3'Calr_{1315–1412} versus neurons treated with LPA + anisomycin and expressing 5'Calr-MyrGFP-3'Calr_{1315–1412} yielded † p = 0.05, †† p = 0.01, and ††† p = 0.001 for time points shown in the graph. By two-way ANOVA compared to t = 0 min post-bleach. **E**, Representative false colored axons showing time-lapse sequences from FRAP analyses of DRG neurons transfected with the indicated plasmids are shown before and after bleaching. The white boxed regions represent the regions subjected to photobleaching and the arrows indicate the regions of the terminal axon where recovery was quantified. **F**, The signals in the series are measured in a 30–50 μ m ROI from the axon tip toward the distal shaft of the cut axon remaining attached to the soma. The quantified signals are normalized to prebleach levels and are expressed as average percent prebleach signals \pm SEM (n = 15 over at least 4 independent transfections). Comparison of DRG neurons co-expressing 5'Calr-Myr-mcherry-3'Calr_{1315–1412} and eIF2 α -S51D versus neurons co-expressing 5'Calr-Myr-mcherry-3'Calr_{1315–1412} and eIF2 α -S51A yielded *p = 0.05, **p = 0.01, and ***p = 0.001 for time points shown in the graph. Comparison of DRG neurons co-expressing 5'Calr-Myr-mcherry-3'Calr_{1315–1412} and eIF2 α -S51D versus neurons co-expressing 5'Calr-Myr-mcherry-3'Calr_{1413–1780} and eIF2 α -S51D yielded †† p = 0.01, and ††† p = 0.001. Comparison of DRG neurons co-expressing 5'Calr-Myr-mcherry-3'Calr_{1413–1780} and eIF2 α -S51D versus neurons co-expressing 5'Calr-Myr-mcherry-3'Calr_{1413–1780} and eIF2 α -S51A yielded p = 0.05 (time points min 18–26), p = 0.01 (time point min 28). By two-way ANOVA compared to t = 0 min post-bleach.

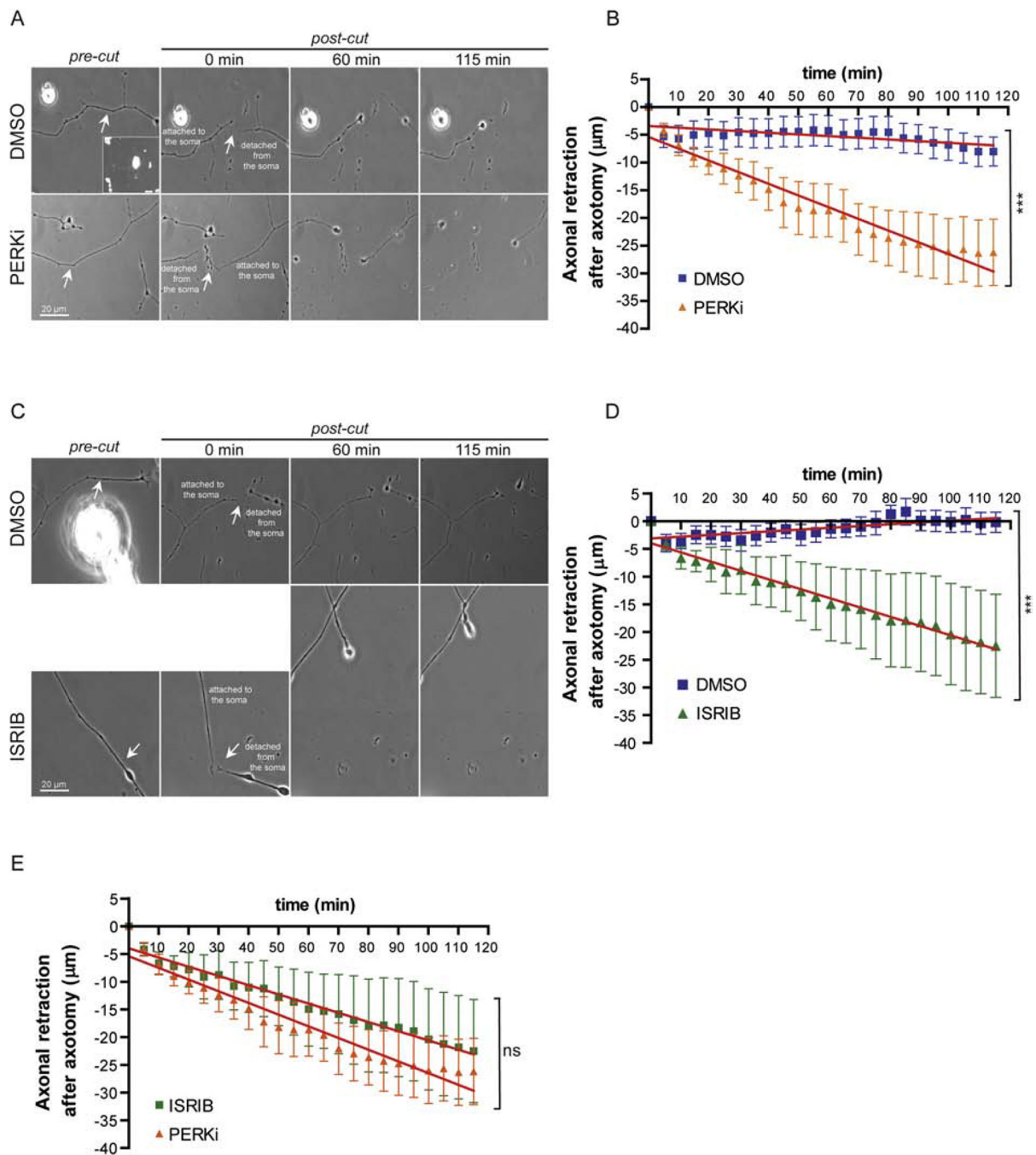


Figure 7. Disruption of eIF2α phosphorylation signaling abolishes the regenerative response of sensory neurons after axotomy.

A, DRG neurons were grown 24 h and pre-treated with PERK inhibitor (GSK2606414, 90 μM) 10–15 min before the axotomy. Representative images are shown before and right after axotomy for PERKi and DMSO treated neurons. The inset panel shows a representative image of a DRG neuron before axotomy (scale bar 50 μm). **B**, The measurement of the axonal position is represented in the graph every 5 min right after axotomy during the 2h time-lapse imaging as an average of the relative distance from the axon tip to the cut site at

each time point \pm SEM ($n = 12$ per each experimental group over at least 4 independent experiments; DMSO $r^2 = 0.4592$, PERKi $r^2 = 0.9401$). Comparison of the regression curve slope of DRG neurons treated with PERKi versus the slope of the regression curve of neurons treated with DMSO yield *** $P < 0.0001$. The axons of DRG neurons treated with PERK inhibitor retracted significantly from the cut site in comparison with the control neurons pretreated with the vehicle. **C**, DRG neurons were grown 24 h and pre-treated with the drug ISRIB (SML-0843, 300 nM) 10–15 min before axotomy. **D**, The measurement of the axonal position is represented in the graph every 5 min right after axotomy during the 2h time-lapse imaging as an average of the relative distance from the axon tip to the cut site at each time point \pm SEM ($n = 12$ for each experimental group over at least 4 independent experiments; DMSO $r^2 = 0.5476$, PERKi $r^2 = 0.9701$). Comparison of the regression curve slope of DRG neurons treated with ISRIB versus the slope of the regression curve of neurons treated with DMSO yield *** $P < 0.0001$. The axons of DRG neurons treated with ISRIB retracted significantly from the cut site in comparison with the control neurons pretreated with the vehicle. **E**, The measurement of the axonal position from DRG neurons treated with both PERKi and ISRIB drugs are compared in the graph as an average of the relative distance from the axon tip to the cut site at each time point \pm SEM ($n = 12$ (PERKi); $n=12$ (ISRIB) over at least 4 independent experiments; DMSO $r^2 = 0.9401$, PERKi $r^2 = 0.9701$). The differences between the slopes of both regression curves were not significantly different ($P > 0.05$).

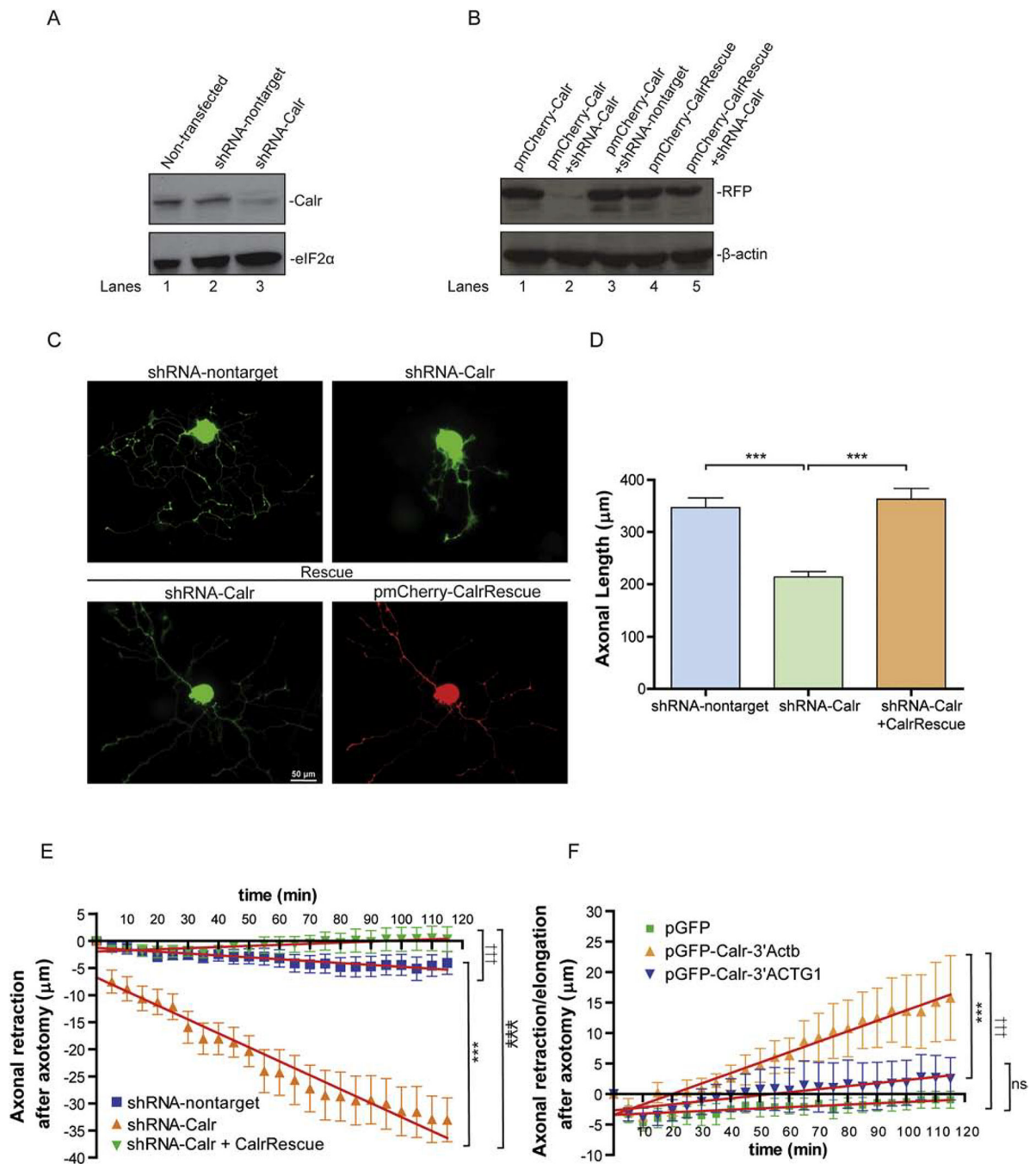


Figure 8. Calreticulin attenuates retraction of injured axons.

A, Western blot panel shows in the first row the knockdown of Calreticulin at 48 h after transfection of F11 cells with the plasmid pSUPERshRNA-Calr-GFP. As a loading control, total eIF2α signal is shown in the second row. **B**, The western blot panel shows in the first lane the decreased endogenous level of exogenous recombinant proteins mcherry-Calr/ mcherry-CalrRescue after co-transfection of F11 cells with the plasmids pSUPERshRNA-Calr-GFP or pSUPERshRNA-nontarget-GFP. As a loading control, β-actin signal is shown in the second row. **C**, Representative static images of DRG neurons expressing shRNA-

nontarget and shRNA-Calr (green panels, first row) or co-expressing shRNA-PERK and mcherry-CalrRescue (green and red panels, second row) are shown 48 h post-transfection. Both mCherry and GFP signals are observed in the cell bodies and in the axons of the neurons. **D**, Axonal length was measured as the longest axon per neuron by tracing the green fluorescent signal of the axons in ImageJ software (NIH) (Donnelly et al., 2011). Quantification of the axonal growth of DRG neurons 48 h after transfection is represented in the graph as the average of axonal length \pm SEM (n = 77 (shRNA-non-target), n = 188 (shRNA-Cal) and n = 89 (shRNA-Cal + CalrRescue)). Comparison of the indicated groups yield ***p < 0.001 by Mann-Whitney test). The axonal length of DRG neurons with decreased endogenous Calreticulin levels was significantly reduced compared to the control neurons. The axonal growth was rescued in DRG neurons co-expressing mcherry-CalrRescue. **E**, The measurement of the axonal position of 48 h DRG cultures expressing shRNA-CAL, shRNA nontarget or shRNA-CAL plus mcherry-CALrescue is represented in the graph every 5 min right after axotomy during the 2h time-lapse imaging as an average of the relative distance from the axon tip to the cut site at each time point \pm SEM (n = 12 for each experimental group over at least 4 independent experiments; shRNA-nontarget $r^2 = 0.7948$, shRNACalr $r^2 = 0.9397$, shRNA-Calr + CalrRescue $r^2 = 0.6630$). Comparison of the regression curve slope of DRG neurons expressing shRNA-Calr versus the slope of the regression curve of neurons expressing shRNA-nontarget yield ***P < 0.0001. Comparison of the regression curve slope of DRG neurons expressing shRNA-Calr versus the regression curve slope of neurons coexpressing shRNA-Calr and CalrRescue yield ~~***~~ P < 0.0001. Comparison of the regression curve slope of DRG neurons expressing shRNA-nontarget versus the slope of the regression curve of neurons coexpressing shRNA-Calr and CalrRescue yield ††† P < 0.0001. **F**, The measurement of the axonal position of 48 h DRG cultures expressing a reporter GFP or an in frame GFP fused to the N-terminus of the rat Calreticulin sequence localized in the axon (GFP-Calr-3' Actb) versus in the soma (GFP-Calr-3' ACTG1) is represented in the graph every 5 min right after axotomy during the 2h time-lapse imaging as an average of the relative distance from the axon tip to the cut site at each time point \pm SEM (n = 10 for each experimental group over at least 4 independent experiments; pGFP $r^2 = 0.4130$, pCalr-3' Actb $r^2 = 0.9660$, pCalr-3' ACTG1 $r^2 = 0.6630$). Comparison of the regression curve slope of DRG neurons expressing GFP-Calr-3' Actb versus the slope of the regression curve of neurons expressing GFP-Calr-3' ACTG1 yield ***P < 0.0001. Comparison of the regression curve slope of DRG neurons expressing GFP-Calr-3' Actb versus the slope of the regression curve of neurons expressing GFP yield ††† P < 0.0001. Comparison of the regression curve slope of DRG neurons expressing GFP versus the regression curve slope of neurons expressing GFP-Calr-3' ACTG1 was not significant (P > 0.05). The axonal elongation of DRG neurons overexpressing the exogenous Calreticulin in the axon (GFP-Calr-3' Actb) was significantly increased compared to the axonal response of DRG neurons overexpressing the exogenous Calreticulin in the soma (GFP-Calr-3' ACTG1) or compared to neurons expressing GFP. However, the axonal elongation of DRG neurons overexpressing GFP-Calr in the soma (GFP-Calr-3' ACTG1) was not significantly different compared to the neurons overexpressing GFP.